Using Site-specific Weather Information and Canopy Sensing to Support Disease Management in Idaho Vineyard

A Thesis

Presented in Partial Fulfillment of the Requirements for the

Degree of Master of Science

with a

Major in Water Resources Engineering & Science

in the

College of Graduate Studies

University of Idaho

by

Dalyn M. McCauley

Major Professor: Jason Kelley, Ph.D.

Committee Members: Alex Maas, Ph.D.; Karen Humes, Ph.D.

Department Administrator: Timothy Link, Ph.D.

May 2020

Authorization to Submit Thesis

This thesis of Dalyn M. McCauley submitted for the degree of Master of Science with a Major in Water Resources Engineering & Science and titled "Using Site-specific Weather Information and Canopy Sensing to Support Disease Management in Idaho Vineyard," has been reviewed in final form. Permission, as indicated by the signatures and dates below, is now granted to submit final copies to the College of Graduate Studies for approval.

Major Professor: _____ Date: _____
Jason Kelley, Ph.D.

Committee Members: _____ Date: _____
Alex Maas, Ph.D.

_____ Date: _____
Karen Humes, Ph.D.

Department Administrator: _____ Date: _____
Timothy Link, Ph.D.

Abstract

Weather dictates farm operations including irrigation scheduling, harvesting, and protection from crop damaging events such as frost, heat waves or disease outbreaks. In a changing climate, it is imperative that farmers are equipped with tools to efficiently and sustainably produce crops with limited resources. Farmers need real-time and site-specific weather data in order to better inform planning and resource allocation. Currently, regional weather networks provide near real-time data in most locations throughout the continental US, but these data may not represent local conditions for most locations. This thesis will focus on the development of low-cost weather stations using the Arduino-platform and describe their application to enhance management decisions in an Idaho vineyard. The low-cost weather stations showed robust results in calibration and were capable of testing rigorous hypotheses about site-specific weather phenomena. As a result, we show how site-specific weather data can answer questions that are directly relevant to disease management. Vineyard canopies are also surveyed using a field spectroradiometer and infrared thermometer to show spatial and temporal patterns of plant physiological response to their environment. A synthesis of socio-economic concerns that may impede the use of weather-based decision support tools is provided, and challenges associated with integrating weather into farm operations are discussed.

Acknowledgements

I would like to acknowledge my academic advisor, Dr. Jason Kelley, for encouraging me to challenge myself and for supporting me through me my graduate education. Results presented in this thesis would not have been possible without help from our field crew, Holly Carter and Danny Baldwin. Lastly, I would like to thank the Meter Group, Inc. (Pullman, WA) for sponsoring the bulk of instrumentation used in this study through the Grant A. Harris Fellowship.

Dedication

This thesis is dedicated to my parents, Jack and Debbie, who instilled in me a sense of curiosity and adventure that has propelled me through my academic journey.

Table of Contents

List of Tables

List of Figures

List of Equations

Chapter 1: Literature Review

The world's rapidly growing population and increased demand for resource intensive crops has put pressure on global food producers. The agricultural sector is a leading consumer of resources, as it accounts for approximately 80% of consumptive water use in the U.S., and is the primary contributor to deforestation and greenhouse gas emissions (Food and Agriculture Organization of the United Nations, 2017; *Irrigation & Water Use*, 2019). The changing climate is expected to exacerbate this with increasing temperatures, changes in precipitation patterns, increased droughts and floods and increased weather variability across local scales (Evans & King, 2012). Weather is intricately intertwined with the agricultural industry as it drives biophysical processes including plant growth, crop water demand, and pathogen development that affect farm operations and productivity. Although climate models predict these changes will be beneficial for some agricultural regions, many arid, Mediterranean and temperate climates are predicted to see changes in crop suitability, decreased yield, and increased water scarcity (IPCC, 2019). Under such climatic stress and uncertainty it is imperative that farmers make informed decisions on resource allocation for the future of sustainable agriculture. This thesis will focus on methods, applications and challenges of integrating site-specific weather and crop data into on-farm decision making.

Information Technology in Agriculture

Information technology and big data are becoming increasingly integral to agricultural production systems. The introduction of global positioning systems (GPS), cheap monitoring technology, and increased computational power have made it possible for farmers to integrate digital information into decision making (Tantalaki et al., 2019). In agriculture applications, the term big data is less associated with the size of the data and more related to the data velocity, variety and veracity (Coble et al., 2018). In other words, big data incorporates high frequency, refined data from multiple sources. Sources of data in agricultural systems have been described to fit into three groups; process mediated, machine generated, and human-sourced (Wolfert et al., 2017). Process mediated data include farm specific business records such as purchasing orders, irrigation records, historical yields, or market and consumer reports. Machine generated data refers to more structured data from sensors, tractors, climate models, or in-season satellite and drone imagery. Lastly, human sourced data incorporates the farmers past experiences and intuition. Big data from some or all of these sources can be employed with machine learning techniques and data analytics to find value from the otherwise disparate sources of information.

Big data can also be used to inform small scale, site-specific decisions, often referred to as Precision Agriculture or Smart Farming Precision agriculture (PA) is defined as a management strategy that uses information technologies to bring data from multiple sources to inform decisions associated with crop production (*Precision Agriculture in the 21st Century*, 1997). Farmers have been making informed decisions on crop management for centuries based on observations, historical outcomes and weather patterns. However, PA is different in that the farm conditions are not assumed homogeneous, and decisions are made from induvial zones rather than the aggregate. In practice, farmers who employ PA techniques utilize site-specific information from sensors, surveys, or aerial imagery to optimize the volume, timing and location of farm inputs such as labor, water, nutrients, or pesticides.

Examples of precision techniques to increase yield or decrease inputs include variable rate irrigation, targeted herbicide applications and pest management, multispectral remote sensing to detect crop nitrogen status, or satellite imagery to predict yield. These tools often promise a competitive advantage for farmers and promote environmental and resource conservation (Sadler et al., 2005). In the last 20 years the adoption of precision agricultural practices such as yield monitoring, variable rate application of inputs and site-specific soil sampling has increased substantially (Griffin et al., 2017). Although there has been an increase in the adoption of some precision agriculture technologies, the use of real-time weather data to inform crop production is less than expected.

Agricultural Weather Networks

Weather data is available to farmers from private and public sources. Public weather data is provided by a variety of agricultural weather networks across the United States. In 2016, there were 28 weather networks containing more than 1600 automated weather stations. Although not all of these are dedicated specifically to agricultural applications, the suite of weather instruments typical at stations were primarily influenced by the need to monitor reference evapotranspiration in the 1980s (Mahmood et al., 2017). Because of this, a majority of automated weather stations provide 5 to 15-minute data of air temperature, relative humidity, incoming solar radiation, precipitation, and wind speed, all of which are directly applicable to farm processes. In the Pacific Northwest Agrimet, AgWeatherNet and the California Irrigation Management Information System (CIMIS) are three agricultural weather networks developed specifically to provide decision support to farmers. These weather networks host automatic weather stations equipped with high quality instruments to provide data products including reference evapotranspiration, degree day models, drought monitoring, severe weather warnings and pest and pathogen development models.

Common instruments found at these stations include air temperature and relative humidity sensors, radiometers to measure incoming solar radiation, anemometers to measure wind speed and direction,

precipitation gauges, soil moisture and temperature sensors, and infrared thermometers (IRT) to measure ground temperature. Each of these measurements are associated with their own set of procedures to maintain accuracy and repeatability, and sensors should be placed such they achieve the following objectives: maximize airflow for naturally temperature and humidity sensors, minimize nearby obstructions to ensure accurate radiation measurements, minimize wind flow around precipitation gauges, maximize distance from tall obstructions (generally a distance of 10 times the height of the nearest tall object), and ensure soils are representative of the surrounding regions (Mahmood et al., 2017). In addition to proper sensor installation, the weather station must also be set up to conform to underlying assumptions of the data products it provides. For example, the measurement of the Penman-Monteith (P-M) reference ET must be taken above a reference surface, which is either a well-watered grass surface maintained at 12cm or a well-watered alfalfa surface maintained at 50cm ("ASCE Manual 70 – Second Edition," 2015). However, conditions at these regional weather stations rarely conform to these requirements.

Though it depends on the individual sensor and data type, generally AgriMet and AgWeatherNet reports weather data every 15 minutes, and CIMIS reports hourly. Data is transmitted every hour from individual stations to a central server where it goes through automatic and manual quality control procedures before being disseminated to the public. The Agrimet QA procedures include checks on data transmission metrics, upper and lower measurement limits, rate of change and a manual graphical review. Additionally, lab calibration is performed on all sensors prior to deployment, and field calibrations are performed annually to ensure the data are reliable and accurate (Palmer & Hamel, 2009). However, agricultural weather stations often go unmaintained, and is important to investigate the quality of the station if utilizing its data.

Weather Related Drivers of Crop Water Use

Increased weather variability and changes in regional weather patterns will substantially impact the hydrological characteristics of basins including the rates of crop evapotranspiration (ET) and the timing and volume of streamflow (Evans & King, 2012). ET is the primary consumptive pathway of water in irrigation systems and is defined as the combined evaporation from bare soil and water vapor transpiration from plants. ET is also directly proportional to crop biomass in well-watered and non-nutrient limited systems (Perry et al., 2009). As such, ET is an important metric for evaluating water use efficiency in agriculture.

As with many agricultural drivers, the rate of evapotranspiration, or crop water use, is highly dependent on local weather. Penman's combination equation derived the physics of evaporation from first principles, describing evaporation in the environment as a product of two factors; the energy

available to maintain evaporation, and the ability of the atmosphere to accept water vapor (Penman, 1948).Using the governing equation of conservation of energy, Penman calculated an energy budget about a well-watered surface where the primary energy source is net radiation. Net radiation is the difference between incoming radiation and outgoing radiation that has either been reflected, emitted or absorbed at the Earth's surface. The primary pathways of the energy left at the surface are in the form of sensible heat, or latent heat, the energy used to for the evaporation of water. The second term in Penman's equation, the ability of the atmosphere to accept water, is based on Fick's law of diffusion. The rate of water vapor flux via diffusive processes is proportional to the concentration gradient, or humidity gradient. In short, water vapor fluxes will move from high to low concentration, such that upward fluxes of water occur when the atmosphere is drier than the surface. Horizontal winds also effect the rate of evaporation such that increased advection will pull away saturated air and replace it with dry air, increasing the atmospheric demand for water. In summary, behind the veil of complex physics, the rate of evaporation depends on solar radiation, air temperature, humidity gradients, and wind speed, all of which can be measured using weather monitoring instruments.

This surface energy budget principle is the basis of modern research and understanding of ET. Later, the original Penman equation was modified by Monteith (1965) to include aerodynamic and surface resistance terms that made it suitable for use in crop canopies. This Penman-Monteith (P-M) reference evapotranspiration (ET_o) equation can be calculated using standard weather data and is the most widely used method for estimating ET in agricultural applications. Reference ET is a measure of the weather-related crop water demand over a well-watered reference surface. Reference ET is not a measure of actual crop evapotranspiration and cannot account for site-specific effects such as non-uniform irrigation, soil characteristics or crop varietal differences. The most common way for farmers to derive actual crop water demand is by adjusting reference ET with a calibrated crop coefficient. Agricultural weather networks provide tables of crop coefficients so that farmers can select the most appropriate for their operations. However, actual circumstances like new crop varieties, differences in timing or differences in plant development are not represented in the provided tables, making it difficult for farmers to choose the correct coefficients for their specific production system. In addition, estimates of crop ET are only as good as the calibrated crop coefficient and applying the wrong coefficient can be a costly mistake for farmers, outweighing the benefits of incorporating ET into irrigation decisions (Davis & Dukes, 2010).

Other methods which measure the actual crop ET include eddy covariance and weighing lysimeters. Eddy covariance (EC) is a technique used to measure turbulent flux of trace gases by high frequency sampling of vertical velocities and scalar air constituent, including water vapor and carbon dioxide.

The covariance between the two measurements over an averaging period is used to derive vertical vapor fluxes from the land surface (Baldocchi, 2014). The primary benefit of using EC is that is in providing an actual measure of ET without disturbing the vegetation or soil. It also provides a spatially representative sample of ET fluxes over an area of hundreds of meters in length. However, because of this large measurement footprint over which EC methods integrate, it is not suitable for measuring individual plants or sub-field scales. The primary drawback to the EC method is the requirement of costly and skilled analysis. Both the instrumentation set up and data processing take skilled personnel, rendering eddy covariance methods costly, time consuming, and often not feasible to achieve in applied settings (Allen et al., 2011a).

Lysimeters are also a direct measure of ET. Lysimeters measure the amount of water lost to ET by weighing the change in water held in an artificial plot of vegetation growing in natural conditions. However, it is challenging to get the conditions within the lysimeter to be representative of the natural conditions. For example, if the surrounding lands are tilled, mimicking that effect in the container can be challenging. Additionally, the crop growth stage, plant rooting depth, and soil profile in the lysimeter needs to match that of the surroundings. For these reasons, the ET obtained from lysimeters values cannot always be directly upscaled to field scales (H. J. Farahani et al., 2007).

Weather Related Drivers of Pathogen Development

An average increase in temperature of 2°C is expected in the next 50 years (IPCC, 2019). This warming is expected to push about 50% of grape growing regions over the climactic threshold of optimum growing conditions. Warmer temperatures have shown to advance development for many grape cultivars by as much as two-weeks (Kornei, 2020), forcing growers to change varieties or change crops entirely (Jones et al., 2005). Development of detrimental fungal diseases such as Powdery Mildew, Downey Mildew and Grey Mold are also highly dependent on weather. Regions with moderate temperatures, increased relative humidity and reduced exposure to UV radiation from the sun are ideal for fungal growth. As such, warming climates in France have already shown to increase disease severity of Downey Mildew in vineyards (Caubel et al., 2013). Second order effects such as wind speed, free moisture from rain, dew or irrigation, and crop evapotranspiration have also shown to impact disease development.

Although grapes are not a water greedy crop, there is still need for irrigation to maintain yield and quality. With the increased likelihood of drought and higher temperatures driving evapotranspiration, it is important to consider all the impacts of increased irrigation. As such, irrigation practices in vineyards might have unforeseen consequences on disease development. Studies have shown that excess irrigation can increase the development of fungal diseases. Austin and Wilcox, (2011) found

that doubling the irrigation rate increased the severity of Powdery Mildew disease by two-fold in a 2007 study and by seven-fold in a repeat study in 2008. This finding was attributed to the increased relative humidity in the leaf boundary layer zone as a result of increased transpiration rates under well-watered conditions. Similarly, a study on strawberry powdery mildew found that well-watered plots had increased disease severity compared to plots that were under deficit irrigation (Xu et al., 2013). For these reasons, enhanced disease detection and warning systems are an important area of inquiry.

Disease Detection Methods

This review will highlight three kinds of disease detection practices, spore traps, weather models, and remote sensing methods, along with their associated advantages and setbacks. First, Thiessen *et al*. (2016) tested the ability of spore traps to be used as on-farm powdery mildew disease detection technique in vineyards. Spore traps are wrapped in a sticky paper and are distributed across fields. The traps are periodically collected, and the spore concentrations are measured using a procedure called Loop-mediated isothermal amplifications (LAMP). The LAMP method determines the airborne concentration of fungi spores in the environment by DNA analysis. They tested the ability for growers to conduct the LAMP tests on-farm compared to laboratory conducted tests and found that there were no significant differences. They also found that pesticide application was reduced when farmers used the spore concentration to inform disease management. One problem with spore traps is that measurements are not accurate during times of low spore concentrations or when there are high background particulates because of the detection limit of the sensor (Thiessen et al., 2016). Although this method is proven to be effective, the practicality of analyzing spore traps on-farm diminishes as the farmer increases the number of traps and the frequency of testing. This is a common trade off with these kinds of sampling procedures.

On the contrary, weather-based models for disease detection provide continuous sampling to inform real-time management decisions. For powdery mildew disease in particular, the UC Davis Powdery Mildew Risk Assessment Index (PMRI) is the most widely accepted tool used to inform pesticide application in vineyards across the western united states (Choudhury et al., 2018). It is used to identify the risk of infection based on a calibrated weather model. The PMRI is broken into two parts, the primary and secondary infection stages. The primary infection is triggered by a 2mm precipitation event followed by 10 hours of leaf wetness under ideal temperature conditions for mildew growth. Once the initial infection is established the secondary phase of the PMRI is used to assess pathogen risk severity throughout the season based solely on air temperature. The PMRI index ranges from 0 – 100 and points are added or subtracted based on a temperature threshold and duration criteria (R. J.

Smith et al., 2019). A study done by Bendek *et al.* (2007) found that using a spray schedule informed by the UC Davis PMRI significantly reduced vineyard disease presence. The recommended spray regime using the PMRI also reduced the number of sprays per season to three compared to five when using the farmer's original, ad-hoc program. Washington State University's regional weather network, AgWeatherNet, provides the daily PMRI index for grape growers in Oregon, Washington and Idaho. The primary problem with this disease detection method is that regional weather data is rarely representative of on-farm weather conditions.

Despite its wide acceptance, Choudhury et al., (2018) highlighted issues with the UC Davis model even when applied to site-specific weather data. First, the model does not account for disease adaptation to high temperatures and does not incorporate other environmental factors such as relative humidity, leaf irradiance, and free moisture that are known to impact the development of powdery mildew. The UC Davis model also does not account for the inherent uncertainty of sensor measurements. Choudhury *et al.* (2018) modified the UC Davis model using a fuzzy logic machine learning process to determine the uncertainty in temperature thresholds that affect powdery mildew development. The fuzzy logic model allowed them to blur the lines of the optimal temperature range and compute a modified PMRI. They found that the fuzzy PMRI model reduced fungicide applications while maintaining comparable disease incidence when compared to the original UC Davis PMRI model. The positive results of this study highlight the effectiveness of using machine learning to recognize patterns in site-specific environmental phenomena that is not fully captured by a single temperature sensor measurement.

Hyperspectral Methods of Detecting Crop Diseases

While local weather information can be used to identify periods of high risk for pathogen development, it cannot provide metrics on actual disease establishment and severity. Hyperspectral remote sensing is an area of research that has become increasingly relevant to agricultural disease detection (Stoll *et al.,* 2018, Bélanger *et al.*, 2008). Hyperspectral remote sensing measures the reflected radiation from a plant resolved into narrow wavebands. The spectral resolution, or band width, of hyperspectral measurements is usually between 1 and 10 nm (Thenkabail et al., 2012). Each band within a hyperspectral signature contains a lot of information on crop physiology; including plant water status, photosynthetic activity, phenological development or disease incidence. The use of vegetation indices (VIs) is a common approach used to reduce the high dimensionality of hyperspectral data, as each hyperspectral signature contains hundreds to thousands of data points. VI's are derived from a combination of bands to identify certain physiological effects that are not obviously apparent.

For example, Šebela *et al. (*2014) inoculated three different grape cultivars with downy mildew and used a field spectroradiometer to measure hemispherical reflectance of the adaxial (top) side of the leaves. They used the Simple Index (SI), which is related to chlorophyll content, and the Carotenoid Ratio Index (CRI_{700}) and found that a decrease in the SI and CRI_{700} vegetation indices correlated with increased disease progress. Rumpf et al. (2010) used support vector machines (SVM) to distinguish between powdery mildew infected sugar beet leaves and healthy leaves during different stages of pathogen growth. Nine vegetative indices derived from non-imaging hyperspectral measurements were used as inputs to the SVM. The accuracy of the supervised SVM model reached 80% at four days after inoculation and 100% after 8 days.

Oerke *et al.* (2016) showed the CRE was able to detect significant differences between healthy grape leaves and leaves infected with Downey Mildew (P. *Viticola*) as early as 9 days after inoculation. Both chlorophyll and carotenoids are leaf pigments that are directly related to photosynthetic potential and can provide information about the physiological stress state of plants. Chlorophyll-a (Chl-a) and Chlorophyll-b (Chl -b) are essential pigments in plants for the conversion of light to energy, as such the plant chlorophyll content can be a direct indicator of photosynthetic activity. Changes in the concentration of photosynthetic pigments such as Chl-a and Chl-b are also known to change with plant-pathogen interactions (Chaerle et al., 2004). For this reason, the use of the chlorophyll vegetation indices as indicators of plant disease have been used in several studies (Erich-Christian Oerke et al., 2016; Rumpf et al., 2010; Šebela et al., 2014). Gitelson *et al.* (2006) found that the best VI for predicting plant chlorophyll content across a range of species is the Chlorophyll Red Edge Index (CRE). The CRE relates the reflectance within the red edge (710nm) to reflectance in the near infra-red (780nm).

$$CRE = \frac{\rho_{780}}{\rho_{710}} - 1$$

Hyperspectral Methods of Detecting Crop Water Stress

Hyperspectral sensing has also been used to identify plant water status in grapevines. There are two primary methods used to identify plant water status. The first method detects changes in plant reflectance in the green wavelengths due to photochemical reactions. Plants absorb more energy from the sun than needed for photosynthesis, so protection mechanisms are used to dissipate excess energy that could be damaging to the plant. One pathway of energy during photosynthesis is via the Xanthophyll pigment cycle. Dissipation of energy from this mechanism within the chloroplast can be observed from reflectance at 531nm (Thenkabail et al., 2012). An increase in light intensity at 531nm corresponds to increased heat dissipation, which is affected by secondary factors such as drought. In

this case, this information can be used to assess plant water stress using the Photochemical Reflectance Index (PRI) (Gamon et al., 1992). The PRI compares reflectance at 531nm to a reflectance at a reference band (usually 571nm) that does not change with photosynthetic activity. More negative PRI values are correlated with increased plant water stress (Thenkabail et al., 2012).

$$PRI = \frac{\rho_{531} - \rho_{570}}{\rho_{531} + \rho_{570}}$$

The second method of detecting plant water status is by measuring the water absorbance of light in the near-infrared region of the spectrum relative to an atmospherics absorption band. Light from the sun passes through the atmosphere as it travels down to vegetation. During this process, light energy at certain wavelengths are absorbed by atmospheric constituents such as water vapor, carbon dioxide, and methane. When light at the wavelength of a water absorption band is incident on vegetation (970nm), the reflected light from the plant will vary slightly depending on the water content of the plant (Peñuelas et al., 1993). The Water Index (WI) developed by Peñuelas *et al.* (1993) compares reflectance at 970nm to reflectance at a reference band that is not as attenuated by atmospheric water absorption, 900nm. This technique is best employed with ground based hyperspectral sensing because additional interaction of light with the atmosphere leads to further absorption and which attenuates the plant's signal.

$$WI = \frac{\rho_{970}}{\rho_{900}}$$

Peñuelas *et al*. (1993) found the WI had a significant linear relationship with relative plant water content, leaf water potential, and leaf temperature depression such that an increase in WI indicated a decrease in plant water content. It was later confirmed by Pôças *et al.* (2017) that the WI is a good predictor for water stress in vines under water deficit conditions. The leaf temperature depression (LTD) can also be used to approximate plant water stress. The LTD is the difference between the air temperature and the apparent canopy temperature, measured using an infrared thermometer. When the plant is transpiring, the canopy temperature will be cooler than the ambient air because of evaporative cooling. Under stressed conditions of limited water and increased air temperatures, plants will regulate their stomata to prevent excessive water loss (Simon et al., 2018). This reduces transpiration, and consequently decreases the latent heat flux, resulting in increased leaf temperatures.

Chapter 2: Low-cost Weather Station Development

Introduction

Weather dictates farm operations including irrigation scheduling, harvesting, and protection from crop damaging events such as frost, heat waves or disease outbreaks. In a changing climate with increased weather variability and water scarcity, it is paramount that farmers are making informed decisions on crop and resource management based on their unique climate. Currently, some farmers have access to regional weather networks that provide near real-time data in most locations throughout the continental US. The problem is that this regional weather data is not representative of on-farm conditions in most locations and does not provide the granularity necessary to make targeted, real-time decisions. Alternatively, farmers may deploy commercial weather stations on their farms that can provide site-specific weather information, though commercial weather systems can be cost prohibitive for small scale farmers. The cost of sensors alone can be expensive, with good quality sensors costing hundreds of dollars. In most on-farm applications, a datalogger is required to query and store information from sensors, which imparts additional costs. As a result, small scale farmers might only be able to afford one or two stations which limits the spatial coverage of weather data and consequently targeted decisions.

Commercial vendors provide a wide range of alternatives, although these vary in quality and in usefulness for on-farm monitoring. Collecting useful environmental data is not trivial. The first step in communicating environmental data is deciding what kind of sensor is needed to capture the physical phenomena of interest. Sensors cannot directly measure precipitation, temperature, relative humidity, wind, etc, but instead measure a change in electrical signal. This signal is in the form of changing resistance, capacitance, current or voltage that occurs as a result of the physical event. Therefore, the sensors should be placed such that they capture the weather parameter of interest, and not some other effect. Even after installation, privately owned weather stations require maintenance to ensure continued accuracy of the measurements. For example, it is recommended that humidity sensors be calibrated every year due to sensor drift. Another issue related to on-farm weather stations is that the data outputs may not be relevant to the farmer's specific needs or in a form that is actionable (Haigh et al., 2018). Dataloggers are often manufacturer specific and only integrate with a narrow selection of sensor types and communication protocols. This limits the flexibility for farmers to customize data outputs to their unique applications, an important factor in the success of on-farm decision support tools (Mase & Prokopy, 2014).

Although there are many interrelated issues with on-farm weather stations, in this project we address the system cost and datalogger customizability. We worked closely with two different decision

makers to develop a customized and low-cost alternative to meteorological data collection that meets their specific needs using an Arduino-based platform. Gunawardena *et al.*, (2018) developed a local energy-budget measurement stations (LEMS) and showed that an Arduino-based weather station could be designed for approximately $1000 USD for use in research applications. The low-cost sensors used for the LEMS had acceptable performance compared to high quality instruments and the LEMS were successfully used in a variety of research studies (Bailey et al., 2016; Gultepe et al., 2016; Hang et al., 2016; Jensen et al., 2017). Others have published similar successes in the development of low-cost weather stations using programmable microcontrollers (Fisher & Gould, 2012; Fisher & Kebede, 2010; Ibrahim Musa, 2018), but the application of low-cost Arduino-based weather stations for use as on-farm tools have not been thoroughly evaluated in the literature. The primary objectives of this project are as follows:

1. Design and build low-cost Arduino-based dataloggers that integrate with a variety of sensor types.
2. Test field robustness and by deploying the systems in two different field studies.
3. Compare a variety of sensors ranging in price to their high-quality counterparts to evaluate the trade-off between sensor accuracy and cost

Methods and Materials

Weather Station Design

The following sections describe the system components in detail. The same datalogger, power system and hardware were paired with different sensors suites for deployment in the two field studies.

Datalogger and Power System

An Arduino MEGA 2560 microcontroller was used as a datalogger. This component is an integral part to the platform due to its high customizability; it can integrate with a variety of sensor types and it is an affordable option to environmental data acquisition. The Arduino MEGA 2560 board is programmed using an open source Arduino software IDE. It hosts 54 digital input and output pins, 16 analog pins, and a 10-bit analog to digital converter. The board was paired with an Adafruit data logging shield equipped with an SD card reader and Real Time Clock (RTC) to synchronize reading and writing data.

The system was powered by a 10W solar panel with an inline charge controller that regulates a 12V battery. It is important that the logger draws as little current as possible to reduce power consumption and maximize battery life under variable sunlight conditions. To reduce power consumption, a library was used to put the board in sleep mode when not taking a measurement. A timer on the RTC

was used to trigger an Interrupt Service Routine (ISR) to wake up the board to take a measurement every 5 minutes. Another feature to reduce power consumption was the addition of an external switching voltage regulator to down regulate the 12V battery to supply 5V DC to the Arduino's input voltage pin to by-pass the internal voltage regulator. The Arduino's internal linear voltage regulator is known to have low efficiency compared to switching regulators (Gjanci & Chowdhury, 2008). As a result of these power system modifications, the system draws 120 mA for one minute while taking a measurement (I_{meas}) and has a current draw of 60 mA in idle (I_{idle}). The 12 V rechargeable battery has a capacity of 5000mAh, which results approximately 6 days of operation with no solar charging, see Equation 1. In full sunlight and partly cloudy conditions, this was ample power supply to run the loggers autonomously.

Equation 1: Weather station power consumption

$$I_{avg} = I_{idle} * \left(\frac{t_{idle}}{t_{total}}\right) + I_{meas} * \left(\frac{t_{meas}}{t_{total}}\right) = 60mA * \left(\frac{240s}{300s}\right) + 110mA * \left(\frac{60\ s}{300\ s}\right) = 70\ mA$$

$$Battery\ Life = \frac{Capactiy}{I_{avg}} = \frac{5000\ mAh}{70mA} = 71\ hours$$

The total cost of the components needed to build and power the datalogger is $138. Table 2.1 shows a price break down of each component.

Table 2.1: Station datalogger and power system components

Component description	**Model**	**Price (USD)**
Microcontroller	Arduino MEGA 2560	$ 40
Datalogging shield	Adafruit Data logging shield	$ 16
10 W Solar panel	Eco-worthy	$ 20
12 V Battery	Power sonic 12V lead acid (5AH)	$ 17
Solar charge controller	MorningStar SunGuard	$ 35
Protoboards, wires, electrical connectors	Misc.	$ 10
	Total cost of logger components:	$ 138

Sensors

The datalogger integrates with sensors that use SDI-12 and inter-integrated circuit (I2C) communication protocols. The I2C communication protocol is common for lower cost digital sensors from hobbyist manufacturers such as Adafruit and SparkFun. These types of sensors come with pre-programmed libraries that are easily compiled in the Arduino IDE. The SDI-12 bus allows for integration with higher quality, more expensive sensors from environmental sensor manufacturers including METER Group Inc., Apogee Instruments and Campbell Scientific. Adding the SDI-12 functionality is not a trivial task, as it entails modifying the pin change interrupt (PCINT) assignments

in the Arduino's internal software serial protocol and the SDI-12 library (Smith, 2014). Compatibility with both the I2C and SDI-12 protocols is an important design feature of this system, as it adds flexibility in the types of sensors that can be used to meet unique applications. A comprehensive list of the sensors that are compatible with this system's circuitry and program can be found in Table 2.2.

Table 2.2: Sensors that are compatible with the low-cost weather station design

Sensor Model	Measurement	Communication protocol	Price (USD)
Sensiron SHT31	Air temperature and humidity	I2C	$16
Melaxis MLX90614	Infrared thermometer (IRT)	I2C	$20
Bosch BMP288/388	Air temperature, humidity and pressure	I2C	$16
Apogee SPI-421	Solar radiation	SDI-12	$285
Decagon GS3	Soil moisture	SDI-12	$225
Decagon MPS2	Soil water potential	SDI-12	$225
Decagon DS2	Wind speed and direction	SDI-12	$550
METER ATMOS 41	All-in-one weather sensor	SDI-12	$1600
METER TEROS 21	Soil moisture	SDI-12	$225
METER TEROS 12	Water potential	SDI-12	$225
METER PHYTOS 1	Leaf wetness	Analog	$125
METER SRS	Spectral reflectance	SDI-12	$325

Enclosures and Hardware

The datalogger, battery and charge controller are housed in a water-tight Pelican enclosure, see Figure 2.1. Cables from the solar panel and sensors come through sealed terminals to connect to the logger. Conduit pipe and fittings were used to build an enclosure for the IRT, see Figure 2.3. A low-cost LaCrosse radiation shield was modified so that the SHT-31 temperature and humidity sensor could be mounted inside. T-slotted 80/20 aluminum struts were used to mount the solar panels and sensors to the enclosure. The hardware used to install the stations in field varied by location.

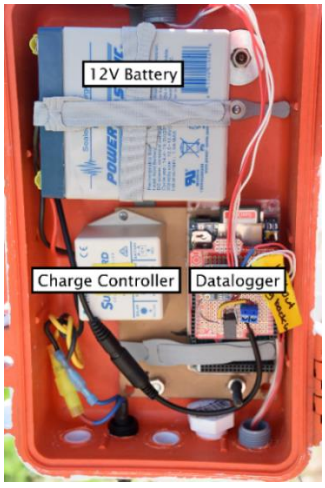

Figure 2.1: Internal set up

Field Deployment Study Design

The weather stations were deployed in two different field experiments. In the experimental designs, we considered things important to producers. The sensors used in the two studies were selected to optimize cost effectiveness and robustness while meeting the accuracy requirements for their unique applications.

Ashton Study

The first experiment was an irrigation study in collaboration with the Henry Fork Foundation (HFF) in Ashton, ID. The HFF was interested in quantifying the differences in evaporative demand between two center pivot irrigation systems: a conventional center pivot with sprinklers at an approximate height of 2 m and a pivot equipped with a Low Elevation Spray Application (LESA) system. LESA systems are intended to increase water efficiency by applying water closer to the canopy and reducing wind losses, but the impact on consumptive water use is unclear. The goal of this study was to assess the potential basin-wide water savings from converting to LESA irrigation in the Henry Fork watershed, a tributary to the Snake River. Only the results related to the station performance will be discussed in this chapter.

The stations were distributed across the two fields such that they capture the upwind, downwind and center field conditions, see Figure 2.2. The sensors used in this study were selected to measure the parameters necessary to calculate the Penman-Monteith (P-M) reference evapotranspiration using an alfalfa reference (“ASCE Manual 70 ", 2015). All stations collected data on 5-minute intervals and measured air temperature, relative humidity and ground temperature.

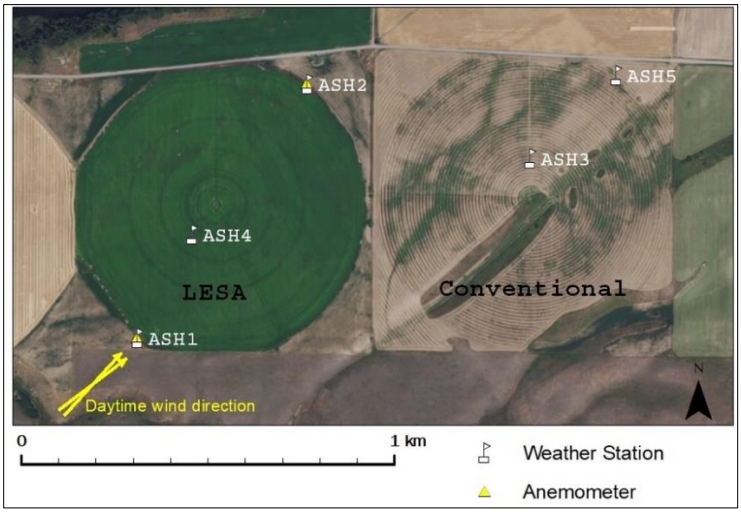

Figure 2.2: Ashton experimental set up

With affordability being the primary design constraint in this study, low cost sensors such as the Melaxis Infrared-thermometer (IRT) and the Adafruit Sensiron SHT-31 were used. These sensors have acceptable accuracy with minimal to no electrical housing which greatly decreases their cost. The upwind station (ASH1) was also equipped with an Apogee SI-421 Pyranometer to measure incoming solar radiation and two R.M. Young cup and vane anemometers were placed downwind from the two fields to measure wind speed and the dominant wind direction. The two stations in the center of the fields also measured soil moisture, soil temperature, and soil matric potential to characterize the soil response to the differing water application rates. Including the datalogger platform and power system, the total cost of a station for this study is between $174 and $473 depending on the sensors used. Table 2.3 describes the sensors and Figure 2.3 shows a typical station set up in the field.

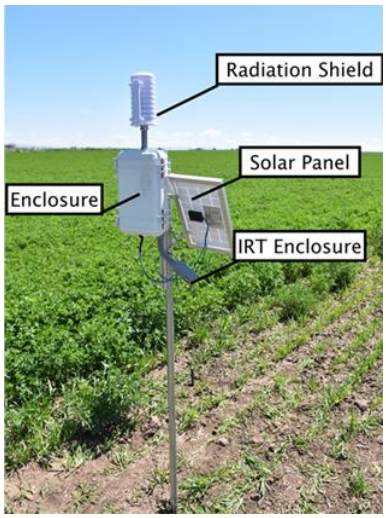

Figure 2.3: Ashton station configuration

Table 2.3: Ashton station sensor details

Sensor Description	Sensor Type	Accuracy	Price (USD)
Air temperature and relative humidity sensor	Sensiron SHT31	± 2%, ± 0.3°C	$16
Infrared thermometer	Melaxis MLX90614	± 0.5°C	$20
Incoming solar radiation	Apogee SPI-421	± 5%	$285
Soil moisture, soil temperature, soil electrical conductivity sensor	Decagon GS3	± 1°C, ± 0.7 m^3/m^3	$225
Soil water potential and soil temperature sensor	Decagon MPS2	± 1°C, ± 0.1 kPa	$225

Vineyard Study

The second field deployment was for a vineyard disease study. A vineyard manager was concerned with Powdery Mildew risk at their vineyard and was interested in a more targeted spray regime to save on labor and chemical costs. Because the vineyard is located across a steep slope at the intersection of two rivers, microclimates are suspected to vary within blocks and across fields. The objective of this study was to determine if there is variable powdery mildew pressure associated with the unique microclimates so that the farmer can optimize the timing, location and intensity of pesticide application. This chapter focuses on the performance of the vineyard weather stations, and a detailed description of the methods and results of this study is provided in Chapter 3.

Figure 2.4: Vineyard station set up

Four weather stations were distributed throughout the vineyard to measure each microclimate. We received a grant from METER Group, Inc (Pullman, WA) that subsidized instrumentation for the vineyard disease study. These stations were equipped with a suite of METER sensors to fully capture the near canopy parameters associated with disease including air temperature, relative humidity, solar radiation, wind speed, soil moisture and leaf wetness, see Table 2.4. These sensors are considered the next level of meteorological sensing technology compared to those used in the irrigation study. Including the datalogger platform, the total cost of a station used in this study is $2557. Although these upgraded sensors increase the unit cost for the vineyard stations, it highlights the expandability of the Arduino datalogger to integrate with a variety of sensor options.

Table 2.4: Vineyard stations sensor details

Sensor Description	Sensor Type	Accuracy	Price (USD)
Infrared thermometer	Melexis MLX90614	±0.5°C	$20
All in one weather station: air temperature, relative humidity, actual vapor pressure, solar radiation, wind speed, wind direction, precipitation, barometric pressure	METER ATMOS 41	RH: ± 0.1% T_{air}: ± 0.6°C Wind Speed: ± 0.3m/s Wind Direction: ± 5°	$1600
Soil water potential and soil temperature sensor	METER TEROS 21	± 1°C, ± 0.1 kPa	$225
Soil moisture, soil temperature, soil electrical conductivity sensor	METER TEROS 12	± 1°C, ± 0.7 m^3/m^3	$225
Leaf wetness sensor	METER PHYTOS 31	± 12 mV	$125
Spectral reflectance sensor	METER SRS	± 10%	$325

Analytical Methods

Calibration Methods

A post-season calibration was done for all stations by placing them adjacent to a high quality, permanent weather station at the University of Idaho's Soil Stewards Farm in Moscow, ID. The five Ashton stations were calibrated for one week in September (9/17/19 – 9/24/19) and the four vineyard stations were calibrated for one week in October (10/02/19-10/09/19). Figure 2.5 shows the calibration set up for the Ashton stations.

Figure 2.5: Calibration set for Ashton stations (Moscow, ID)

Temperature and humidity measurements from the ATMOS 41, and SHT 31 were compared to their higher quality counterpart on the permanent weather station, an Elektronic EE180 temperature and humidity sensors. Linear regressions between the low-cost station sensors and their corresponding sensor on the permanent weather station were used to determine calibration equations.

Results

Weather Station Performance in Field

The Ashton weather stations were in the field for a total of 75 days between June 6th, 2019 and August 21st, 2019. Figure 2.6 shows the periods of data collection for each station. Shortly after the stations were deployed in June, all the data loggers shut off due to a communication error with the MLX90614 IRT. After this initial issue, ASH1, ASH2 and ASH3 ran relatively consistently. ASH 4 and ASH5 continued to have problems with sensor communication errors through July which froze the program. It was later identified during a field visit in July that the SHT-31 sensor on ASH5 had died, and the IRT on ASH4 was flooded from the overhead irrigation.

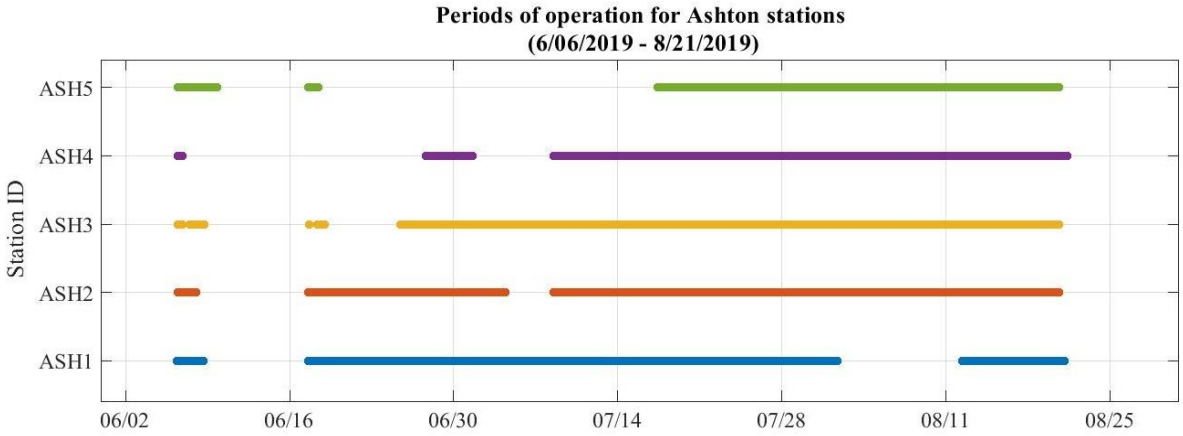

Figure 2.6: Periods of operation for Ashton stations. Solid lines indicate periods of data collection for each station.

The vineyard stations S1, S2 and S3 ran for a total of 135 days from May 1st to September 13th. Station 4 was installed on May 8th and ran for a total of 127 days. These stations performed relatively well compared to the Ashton stations, Figure 2.7. There were some datalogger drop-outs shortly after deployment for S2 and S4. This issue was found to be due to a wiring fault in the RTC clock, such that the datalogger would not wakeup from sleep mode. All logger shields were remade and replaced, and the stations performed consistently thereinafter. The dropouts of S1, S2 and S3 in early July were due to depleted batteries from lack of solar charge as the vineyard canopy grew over the solar panels. Despite these hiccups, when the power system and timers operated correctly, the weather stations performed consistently.

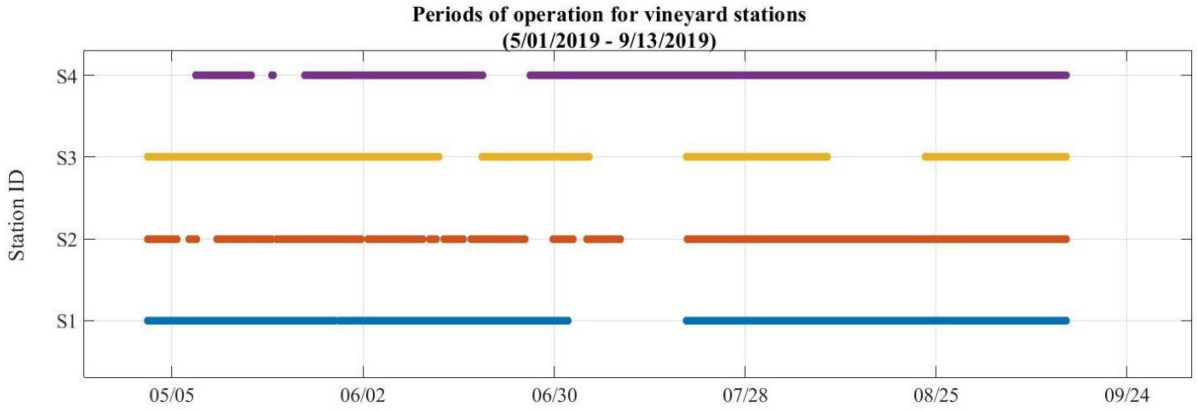

Figure 2.7: Periods of operation for vineyard stations. Solid lines indicate periods of data collection for each station.

Calibration Results

The calibration results from the ATMOS 41 all-in-one weather station showed good agreement with the permanent weather station's Campbell Scientific EE-180 Temperature and Humidity sensor, Figure 2.8. The air temperature measurements had an average r^2 of 0.9985, which is nearly perfect agreement. See Table 2.5 for the linear regression results for each station.The range of temperatures observed during calibration (-3°C – 20°C) did not capture the full range of the sensor temperature specification (-40°C – 50°C), nor the full range observed in the field experiment (-10°C – 45°C), so it is not certain that the sensor performs linearly across all temperatures.

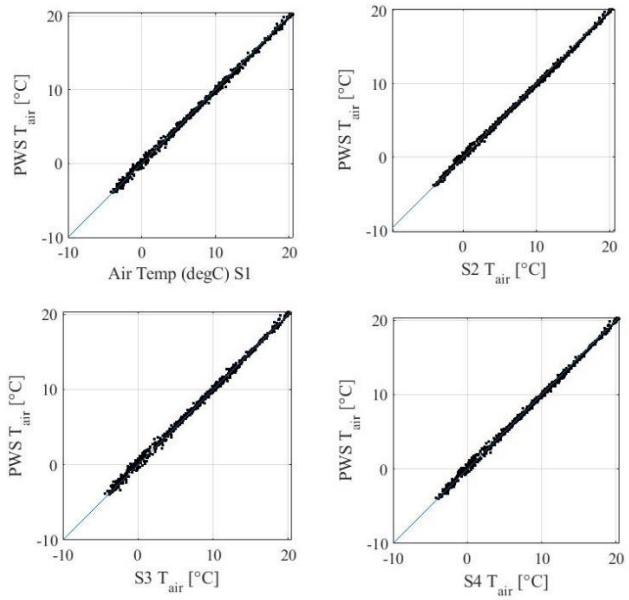

Figure 2.8: Post-season calibration results for temperature measurement from ATMOS-41 sensor on vineyard weather compared to EE-188 HMP temperature sensor on permanent weather station (PWS) at the University of Idaho's Soil Stewards Farm (10/02/19-10/09/19)

Table 2.5: Regression equations between ATMOS-41 and PWS for air temperature measurement

Station ID	R-square	Intercept	Slope
S1	0.9984	0.0404	0.9851
S2	0.9989	0.0317	0.9843
S3	0.9980	0.1771	0.9859
S4	0.9985	0.0931	0.9830

The relative humidity measurements from the ATMOS-41 were not in perfect agreement with the humidity measurement from the EE-180, Figure 2.9. The ATMOS-41 measurement tended to overestimate the relative humidity of values above 70% though an average r-square of 0.9715 still shows excellent agreement, Table 2.6.

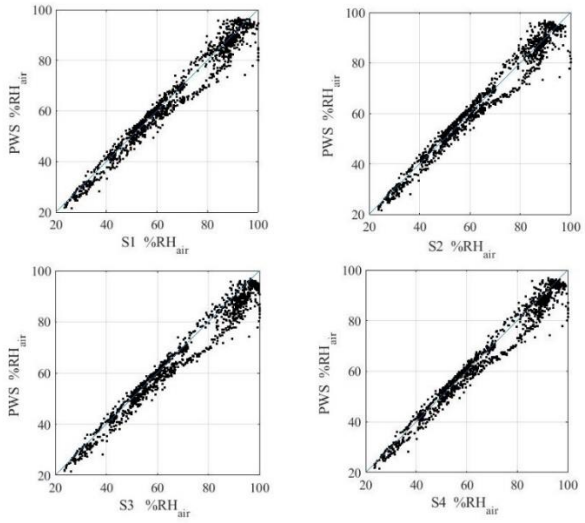

Figure 2.9: Post-season calibration results for humidity measurement from ATMOS-41 sensor on vineyard weather compared to EE-188 HMP humidity sensor on permanent weather station (PWS) at the University of Idaho's Soil Stewards Farm (10/02/19-10/09/19)

Table 2.6: Regression equations between ATMOS-41 and PWS for relative humidity measurement

Station ID	R-square	Intercept	Slope
S1	0.9691	0.1127	0.9755
S2	0.9696	0.0115	0.9936
S3	0.9726	2.4916	0.9253
S4	0.9747	1.7102	0.9526

The lower cost SHT-31 temperature and humidity sensors used in the Ashton study were less accurate when compared to the high-quality sensors on the permanent weather station with an average r-square of 0.9583 and 0.9598, respectively. Table 2.7 and Table 2.8 give the linear regression results for the temperature and humidity measurements, respectively. The SHT-31 temperature sensors tended to overestimate the air temperature, and consequently the humidity sensor tended to underestimate the relative humidity, Figure 2.10 and Figure 2.11. There is also hysteresis observed in the SHT-31 temperature and humidity measurement. Hysteresis occurs when there is a lag in the measurement

response to the changing temperature and is often due to the response time of the sensor, or the response time of the radiation shield.

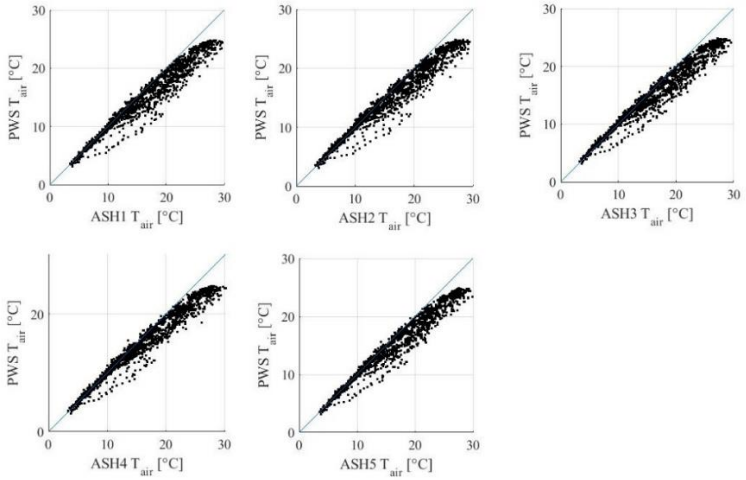

Figure 2.10: Post-season calibration results for air temperature measurement from low cost SHT-31D sensor on Ashton weather station compared to EE-188 HMP temperature sensor on permanent weather station (PWS) at the University of Idaho's Soil Stewards Farm (9/17/19 – 9/24/19)

Table 2.7: Regression equations between SHT-31 and PWS for air temperature measurement

Station ID	R-square	Intercept	Slope
ASH1	0.9526	1.465	0.8219
ASH2	0.9559	1.632	0.8237
ASH3	0.9580	1.736	0.8180
ASH4	0.9642	1.597	0.8234
ASH5	0.9607	1.517	0.8239

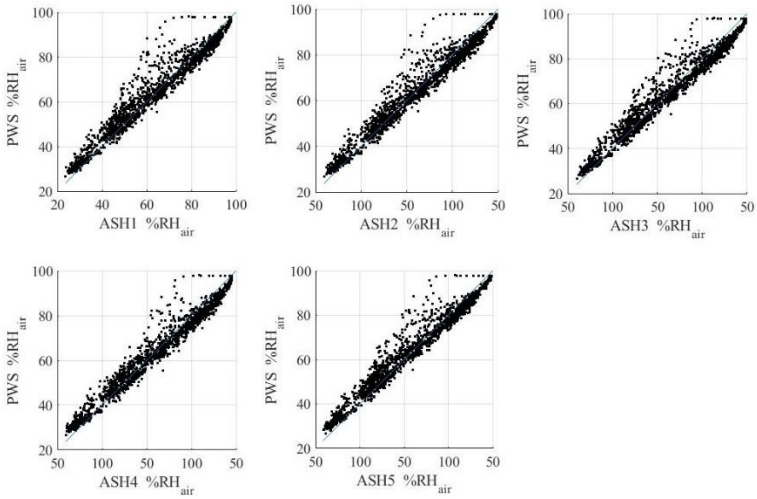

Figure 2.11: Post-season calibration results for relative humidity measurement from low cost SHT-31D sensor on Ashton weather station compared to EE-188 HMP humidity sensor on permanent weather station (PWS) at the University of Idaho's Soil Stewards Farm (9/17/19 – 9/24/19)

Table 2.8: Regression equations between SHT-31 and PWS for relative humidity measurement

Station ID	R-square	Intercept	Slope
ASH1	0.9521	7.526	0.8919
ASH2	0.9589	6.821	0.8904
ASH3	0.9604	7.095	0.8838
ASH4	0.9667	6.666	0.8912
ASH5	0.9610	8.439	0.8798

Figure 2.12 shows how the temperature error changes over the course of the day, calculated as the difference between SHT-31 temperature measurement and the EE-180 temperature measurement on the permanent weather station (PWS):

$$Temperature\ Error = T_{SHT31} - T_{PWS}$$

Figure 2.13 shows how solar radiation changes over the course of the day. Comparing these two plots shows that the sensor error is greatest during the day, particularly in the morning (7:00 – 12:00). Error is minimal, less than 0.5°C, when the sun is down, indicating that the sensor bias may be due to the lower quality radiation shield, and not the sensor itself.

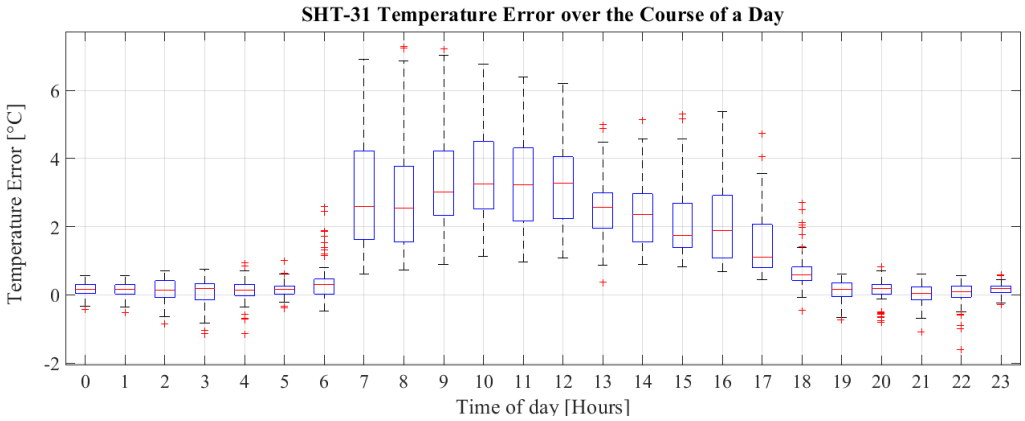

Figure 2.12: SHT-31 temperature error over the course of the day

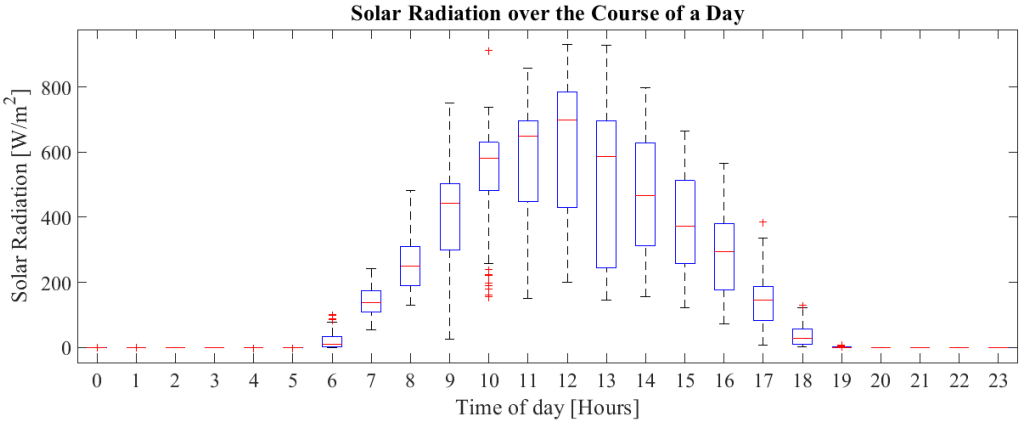

Figure 2.13: Solar radiation over the course of the day

Figure 2.14 shows a matrix of the air temperature agreement between the five SHT-31 sensors. These plots show that the individual sensors are in excellent agreement. This indicates that a single calibration equation could be used to correct all sensors. Assuming the EE-180 sensor represents the true temperature and relative humidity, a calibration equation can be derived from the average slope and offset observed under the field conditions, see Equation 2. The calibration set up was performed under natural conditions and was not conducted in an environmental chamber. Because of this, the sensors were not exposed to their entire measurement range, nor were they exposed to abrupt step changes in temperature and humidity. This correction equation is specific to the conditions observed during the calibration, and only applies in the temperature range of 5-30°C.

Equation 2: SHT-31 temperature correction for the range of 5-30°C

$$T_{corr} = \frac{T_{PWS} - 1.589}{0.8222}$$

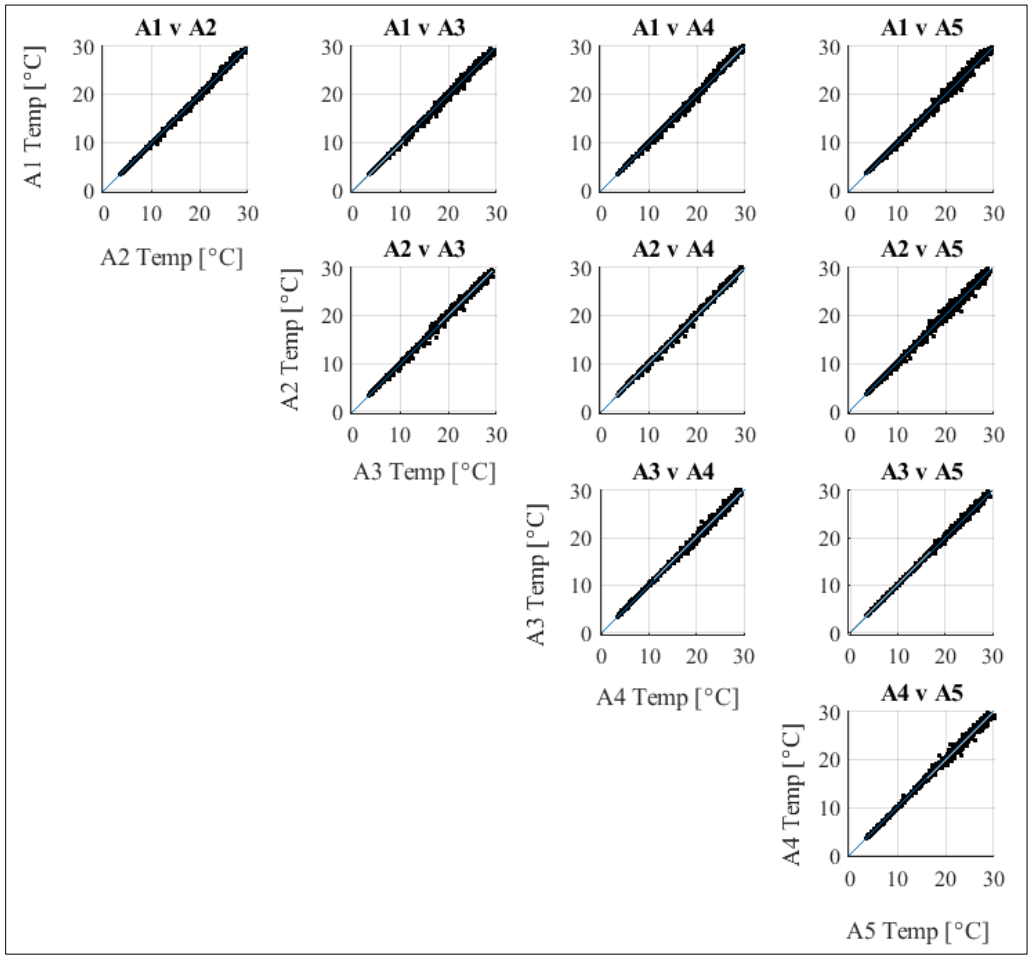

Figure 2.14: Sensor to sensor agreement for SHT-31 temperature

Discussion

Overall, the weather stations performed well in the two field experiments. The weather station power system and RTC communication were the two primary causes of problems in the field. For the vineyard stations, mid-season drop-outs were clearly related to canopy growth covering the solar panels. During a July field visit, the canopy was covering approximately 80% of S1, S2 and S3 solar panels. This blocked a significant amount of radiation so that the battery was not charging fast enough to keep up with the power consumption of the loggers. In this case it was an easy fix to cut back the canopy, but this highlights the sensitivity of solar powered system. Solar powered weather stations might not be an acceptable option in regions with frequent cloud cover, in locations that are experience a lot of shade, or during fall and winter seasons with minimal daylight hours. The communication errors with the I2C sensors (IRT, SHT-31 and RTC) in the both experiments highlight the complexity of logging sensor data. The issue with the RTC in the vineyard experiment was due to a simple circuit mistake. When a data line is not pulled up to a constant voltage via a resistor it is called a floating signal. Floating signals can cause intermittent, and unpredictable malfunctions in the system, making it difficult to troubleshoot. These are the types of issues that can arise with low-cost and DIY systems that inhibit people from using this as an option for on-farm weather data.

The labor associated with building and maintaining these low-cost weather stations should also be factored into the overall cost. For example, the stations used in the vineyard study cost $2557 each, and each station took approximately 8 hours to build, and 1.5 hours to install. We estimate that the time spent maintaining the station totals to 30 minutes a month for each station, and an additional 45 minutes per station was included for the uninstallation at the end of the season. All the labor was billed for a typical farm worker, except for the labor for building the weather stations, which was billed at the approximate rate of a research scientist. Table 2.9 shows an estimate of the labor and maintenance costs associated with installing an on-farm weather station.

Table 2.9: Labor and maintenance cost breakdown for vineyard weather stations

Cost	Time (hours)	Price (hourly)	Units	Frequency	Cost
Station maintenance labor	0.50	$ 10	1	6	$ 30
Installation labor	1.5	$ 10	1	1	$ 15
Building labor	8	$ 23	1	1	$ 184
Uninstallation labor	0.75	$ 10	1	1	$ 7.5
				Total/Station	**$ 236.50**

To assess the value of these weather stations, we compare the weather station investment to potential economic losses from a severe powdery mildew infection. Table 2.10 shows a range of scenarios for vineyard revenue depending on the grape type (red or white), quality (price/ton) and yield (tons/acre). The table also shows the potential loss in revenue from a disease outbreak, where we assume that a powdery mildew outbreak will decrease the yield by 12% and decrease the fruit quality by 10% as supported by the literature (Calonnec et al., 2004). For a vineyard that has an average yield for the state of Idaho, 4 tons/acre, and produces grapes of average quality ($1050/ton for white grapes and $1400/ton for red grapes), we estimate that the average revenue loss from a disease outbreak could be $1835/acre.

Table 2.10: Revenue for six vineyard production scenarios and the associated losses in the event of a disease outbreak. For these scenarios, a disease outbreak is assumed to reduce yield by 12% and reduce the price/ton by 10%.

Grape	Price/Ton	Tons/Acre	Revenue/Acre	Revenue Loss from Disease/Acre
Red	$ 1,200	2	$ 2,400	$ -900
Red	$ 1,400	4	$ 5,600	$ -2,100
Red	$ 1,600	6	$ 9,600	$ -3,600
White	$ 900	2	$ 1,800	$ -700
White	$ 1,050	4	$ 4,200	$ -1,570
White	$ 1,200	6	$ 7,200	$ -2,700

Table 2.11 shows the cost breakdown for disease management, including the cost associated with incorporating weather stations. For this assessment, we show the cost of installing four weather stations in 35 acres of vineyard. We assume that these weather stations have a service life of 5 years. The capital investment of the weather stations, including the material costs and labor costs of building, is divided evenly across the five years. For simplicity, the time value of money was neglected in this analysis. The cost of disease management includes the material, labor and maintenance associated with fungicide application. A case study of a vineyard in the San Juaquin Valley, CA found that there is an initial cost of $46/acre, and an additional cost of $34/acre for each fungicide application to manage powdery mildew (Fidelibus et al., 2018). For this analysis, we assume that the vineyard applies fungicide bi-weekly, for a total of 8 applications from April through July.

Table 2.11: The costs associated with disease management

Disease Management Costs	Price/Acre	Frequency/Year	Cost/Acre
Pesticide Material & Labor Cost			
Pesticide Primer	$ 46.00	1	$ 46.00
Pesticide Application	$ 34.00	8	$ 272.00
		Total:	**$ 318.00**
Station Maintenance & Labor Cost			
Station Maintenance	$ 0.29	12	$ 3.43
Station Installation	$ 1.71	1	$ 1.71
Station Un-installation	$ 0.86	1	$ 0.86
		Total:	**$ 6.00**
Capital Investment			
Station Building Labor	$ 21.03	1	$ 4.21
Station Capital Cost	$ 292.23	1	$ 58.45
		Total:	**$ 62.65**
		Total cost per year/Acre	**$ 386.65**

We found that the cost of disease management including weather information is approximately $387/acre per year. This is about a fifth of the cost of decreased yield and fruit quality as a result of a powdery mildew disease outbreak. Given that the weather data This simple comparison shows that the potential losses from disease far outweigh the cost of using weather data to help inform the timing and location of disease risk.

A more qualitative metric of the stations' performance is the ease of use for the operator. For the vineyard stations, a lab tech and myself were the only ones who downloaded data from the SD cards. This process is relatively straight forward when the stations are operating, simply remove the SD card, load it onto a computer and put it back into the logger. Though this operation was not as seamless for the stations in Ashton, ID, especially when they had malfunctioned. Our collaborator at HFF primarily operated the stations in Ashton, aside from our three field visits. He found that troubleshooting the systems was challenging and downloading the data directly from the SD card was inconvenient. This highlights two primary areas for improvement. The first is that the weather data needs to be transmitted over telemetry or Wi-Fi for these stations to be practical on-farm tools. For farms that do not have easy access to Wi-Fi or cellular service, this becomes an added cost. The second area of improvement is the user interface at the logger itself. Ideally, it would be possible to troubleshoot the systems in the field without a computer. This functionality would require an LCD display, some input buttons, and add a great deal of complexity to the program. Though these two features are available for some dataloggers on the market, they are not standard, and it is important to recognize the factors that inhibit farmers from collecting and using site specific weather data.

The sensor comparison to the high-quality meteorology instruments showed acceptable agreement. The more expensive ($1600) ATMOS-41 had a nearly identical response to the EE-188 HMP temperature measurement. Due to design constraints the ATMOS-41 temperature sensor is not contained in a radiation shield as typically required for air temperature measurements. The sensor is partially exposed to radiation resulting in measurement errors, but because the ATMOS-41 also measures solar radiation and wind speed, the instrument performs a correction using a simple energy balance (*ATMOS 41—Correction of Air Temperature Measurements from a Radiation-Exposed Sensor*, n.d.). The positive results of this calibration indicate that this correction is sufficient to regain a precise air temperature measurement.

The SHT-31 temperature and humidity sensor did not perform as well in calibration. The sensors tended to overestimate the temperature and underestimate the relative humidity. Because the sensor to sensor agreement was so strong, this bias could be corrected in all sensors using a single linear regression equation. The hysteresis observed in the SHT-31 measurements could be attributed to the time response of the SHT-31 sensor, or the time response of the radiation shield. The time response of the temperature and humidity measurement are 2 seconds and 8 seconds, respectively. However, the lags were observed across five-minute sampling intervals, indicating that the hysteresis is not a product of the sensor's time response. Instead, the lags could be due to the time response of the radiation shield. The time response of a radiation shield is related to ventilation. The greater the ventilation, the quicker the temperature sensors are exposed to the changing air temperature. Whereas limited ventilation allows air to stabilize near the sensor and warm. This could result in a biased measurement which is lagged behind the measurements from the permanent weather station which has a higher quality radiation shield. Similarly, for the relative humidity measurement, an increase in the thermal mass of the air due to poor ventilation would result in a decreased relative humidity measurement.

Though the calibration results of lower cost ($16) SHT-31 sensors were not as accurate as the ATMOS-41, an average r-square of 0.95 and 0.96 for relative humidity and temperature measurements is still very accurate. Although it depends on the farmer's specific needs, the accuracies of the low-cost sensors should be more than adequate to improve decision making. When considering the alternative of farmers using data from regional weather stations to track growing degree days or reference evapotranspiration, this on-farm measurement is a much more useful and representative despite its lower quality.

Chapter 3: Powdery Mildew Study

Introduction

One of the major threats to production in agriculture are plant diseases and pests. A 2017 FAO report estimated that as much as 20 - 40% of global food production is lost to plant diseases (*Plant Health and Food Security*, 2017). Grape powdery mildew (*Erysiphe necator*) is one of the most persistent disease problems facing wine grape producers in the western united states (Choudhury et al., 2018). In the case of an outbreak, powdery mildew can be detrimental to growers in the form of yield losses and decreased fruit quality. A study conducted in the Bordeaux region of France found that diseased berries of Cabernet Sauvignon had an average reduction in weight of 12% and 20% in 1997 and 1999 studies, respectively (Calonnec et al., 2004). Severe infections may require entire vineyard blocks to be uprooted and replanted leading to years of regrowth before the vines can be productive again. Both Calonnec et al. (2004) and Gadoury et al., (2001) saw significant increases in sugar content and decreased brix values in infected fruit. These changes to fruit biochemistry can lead to noticeably decreased wine quality. Stummer et al. (2005) showed degradation of sensory and compositional characteristics of wine when made with less than 5% powdery mildew infected berries. In addition to decreased yield and quality, even a diffuse or mild powdery mildew colonization increases plant susceptibility to other damaging threats including bunch rot and insect infestation (Gadoury et al., 2007).

Producers use a variety of techniques to reduce losses to pests and plant pathogens including crop rotations, tillage and hoeing, adjustment of planting dates or biocontrol. The most common tool for pest and disease management in vineyards is use of chemical pesticides. An increase in the variety of pesticides available on the market today has expanded the range of control growers have for pathogen management, but it comes at a cost. Pesticide applications are expensive, labor intensive, and environmentally destructive. In the US alone, over $12 billion was spent on pesticides to manage crop disease in 2008. Grapes are reported as one of the top 21 crops contributing to pesticide usage, accounting for 1.5% of the total (Fernandez-Cornejo *et al.*, 2014). This degree of pesticide use poses a significant threat to water quality. Runoff from vineyard catchments have been shown to contribute substantially to pesticide loads entering erosion rills, streams and even ground water, pushing some waters over the maximum allowable limits (Hildebrandt et al., 2008). Plant pathogens have also become more resistant to certain chemicals in pesticide formulas when used continuously and exclusively, which poses a threat to the effectiveness of pesticides and consequently agricultural yields in the future (E.-C. Oerke, 1994). Climate change is expected to exacerbate the problem because both pathogen development and pathogen resistance have been shown to develop more

rapidly with increased temperatures (Caubel et al., 2013; Chakraborty et al., 2000). For these reason, informed disease management and methods to reduce pesticide applications are important areas of inquiry for the future of sustainable agriculture.

A vineyard manager in Northern Idaho was interested in better understanding the timing and spread of Powdery Mildew outbreaks in their vineyard. Currently, the grower's disease management is ad-hoc; applying fungicide every two-weeks, or whenever operations permit. With a new atomized sprayer that greatly improves fungicide coverage within the canopy, the farmer is interested in a more targeted spray regime to save on labor, chemical costs, and limit the pesticide exposure for the environment and workers. The goal of this study is to better inform the timing and location of fungicide spray. In particular, I aim to investigate if powdery mildew disease pressure in an Idaho vineyard significantly varies in time and space using distributed weather stations and hyperspectral canopy sensing.

Powdery mildew is fungal disease that is highly depended on weather. It survives the winter as dormant mycelia and ascospores are released in the spring with rainfall, irrigation or fog. Initial infection occurs once temperatures reach an optimum, between 18 – 30°C, and production of fungal spores begins approximately a week after and continues throughout the season (Gubler *et al.*, 1999). Air temperature has a first order effect on the rate of fungal germination throughout the season, ergo common disease management strategies are based on daily temperature, like the UC Davis Powdery Mildew Risk Assessment Index or pathogen growing degree days. However, other weather parameters are known to impact the development, germination and dispersal of powdery mildew. Bendek *et al*. (2007) conducted a study in Chile where they inoculated chardonnay in a greenhouse with powdery mildew to determine the effect of temperature, relative humidity (RH) and free moisture on spore development. They found that germination increased at RH greater than 33-35% when incubated at 20°C and germination was highest when the conidia were subject to 24 hours of dry followed by 24 hours of wet leaf conditions. A study on Hop Downey Mildew showed that increased wind speeds in the near canopy boundary layer agitated fungal spores and facilitated transport to increase the spread of disease (Mahaffee & Stoll, 2016). Because there are a myriad of environmental conditions and combinations that can influence the development and spread of powdery mildew, it is important to identify differences in microclimates across the vineyard to inform potential management zones. Consequently, the primary research question addressed in this study:

1. Are there detectable differences in temperature, relative humidity, and windspeed distributions across the vineyard that impact disease susceptibility?

Studies have also shown that near canopy moisture from plant transpiration can impact powdery mildew development. Austin and Wilcox, (2011) found that doubling the irrigation rate increased the severity of Powdery Mildew disease in a French vineyard by two-fold in a 2007 study and by seven-fold in a 2008 study. This finding was attributed to the increased relative humidity in the leaf boundary layer zone as a result of increased transpiration rates under well-watered conditions. On the contrary, studies have also found that grapevines under increased water stress are more susceptible to disease (Stoll et al., 2008; van Niekerk et al., 2011). As such, it is important to characterize vineyard transpiration and water stress when investigating disease pressure, motivating the second research question addressed in this study:

2. Are there detectable differences in plant water stress and transpiration rates across the vineyard?

Lastly, remote sensing technologies are becoming increasingly integrated in pest management. There has been ample research on disease detection methods using multi and hyperspectral remote sensing techniques (Marshall et al., 2016; Erich-Christian Oerke et al., 2016; Rumpf et al., 2010; Stoll et al., 2008). These studies have described features of plant hyperspectral signatures that can be used for early detection of disease presence in grape leaves under lab environments (Stoll *et al.*, 2018, Bélanger *et al.*, 2008), but limited research has incorporated field based, non-imaging hyperspectral sensing for powdery mildew disease detection. This is an important distinction when considering implementing technology into on-farm practices, and leads to the third research question:

3. Are field-based methods of hyperspectral canopy sensing able to identify the presence of grape Powdery Mildew disease?

Methods and Materials

Study design

Site Description

The study site is a vineyard in Juliaetta, Idaho, where managing the risk of powdery mildew is a concern of the grower. The nearly 30 acres of vineyards are located across a valley at the interception of the Potlatch River and the Clearwater River. The vineyards are steeply sloped and distributed across areas with different solar aspects indicating inherent heterogeneity of microclimates. All vineyard soils are primarily an ashy silt-loam with high water holding capacity (NRCS, 2017). Two modes of data collection were employed to capture both the temporal and spatial characteristics impacting susceptibility to disease. The first was use of distributed weather stations to continuously monitor local differences in micro-climates over time, see Figure 3.1 for site map and station locations. The second mode of information was obtained by conducting bi-weekly canopy surveys to characterize the spatial variability of microclimates and plant stress across vineyard rows using measurements of near canopy climate and canopy hyperspectral radiance.

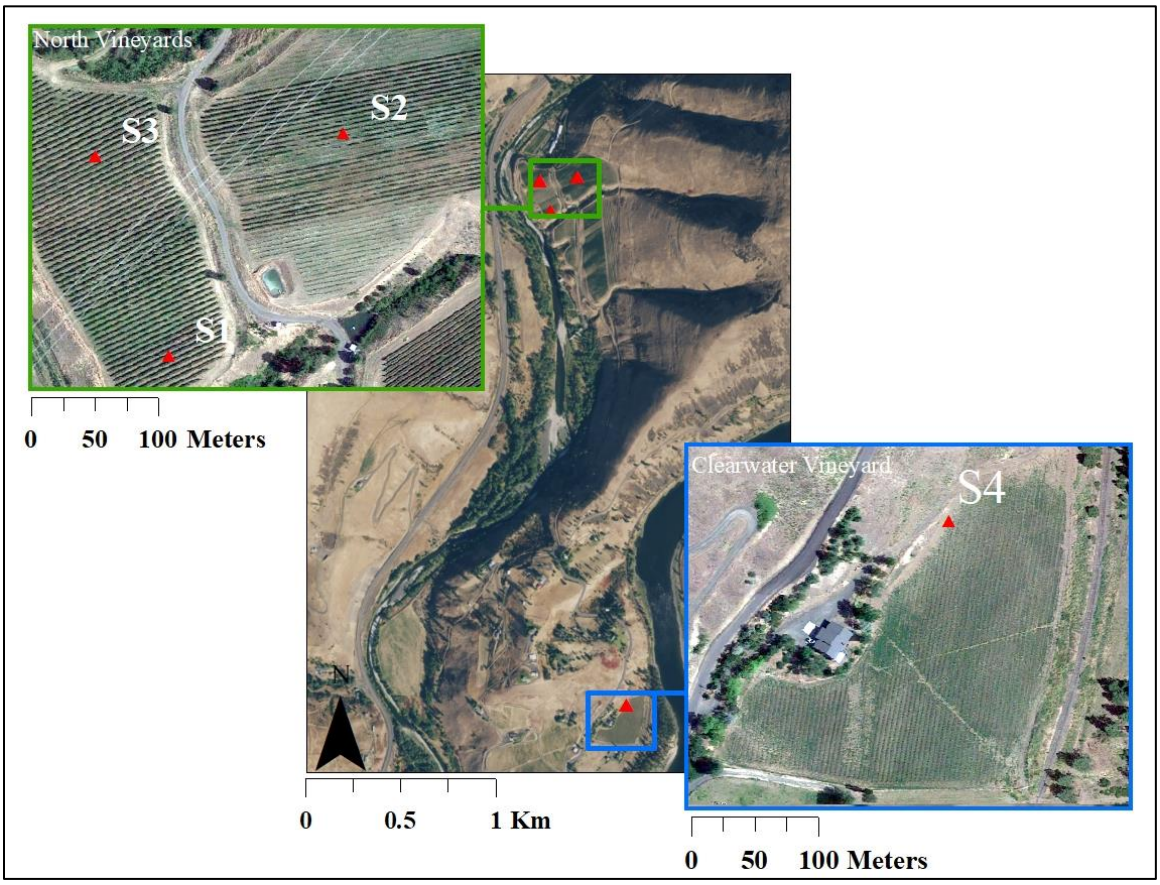

Figure 3.1: Site map across ridge; North vineyards are located on a west facing slope, and the clearwater vineyard is located on a southeast facing slope (Julieatta, ID)

Distributed Weather Stations

Four weather stations were distributed throughout the vineyard to measure environmental factors associated with the infection and spread of powdery mildew. Stations were mounted on existing T-posts in the Chardonnay, Riesling, Grenache and Syrah varieties which are referred to as S1, S2, S3 and S4, respectively. The station locations were chosen to monitor areas where disease had been present historically while capturing a range of microclimates, see Figure 3.2.

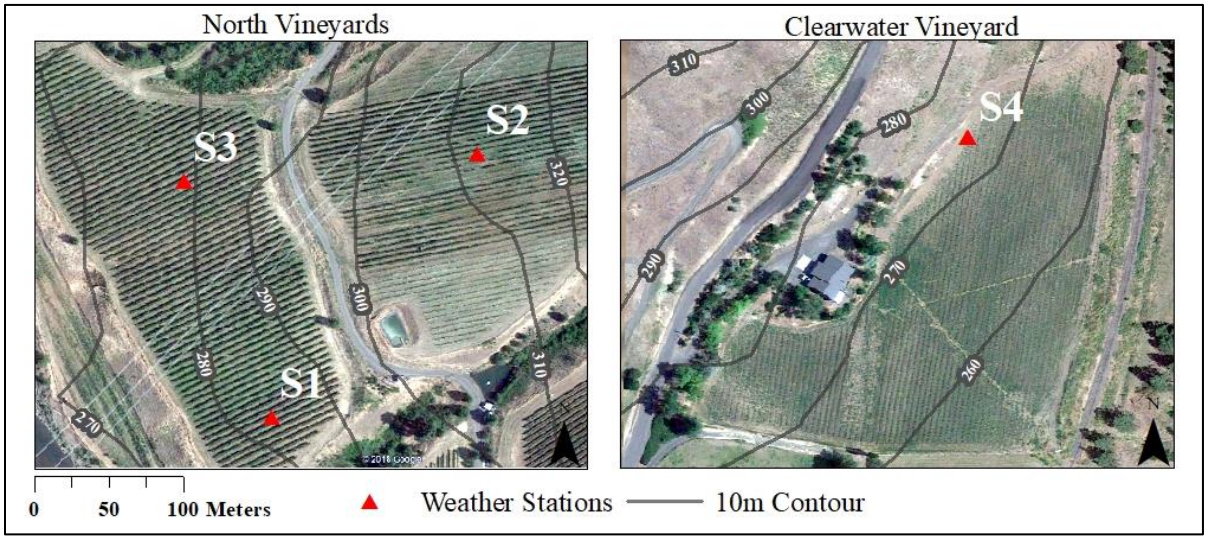

Figure 3.2: Station locations across vineyard, S1 (Chardonnay), S2 (Grenache), S3 (Riesling), and S4 (Syrah)

The vineyard manager indicated that the Chardonnay variety surrounding S1 has been the first area to become symptomatic of powdery mildew in the past. He noted that the infection would later show up in the Riesling plants surrounding S3. For this reason, it was important to monitor the weather in both locations within this vineyard block to assess potentially differences that could lead to the lagged initial infection. To determine the range of microclimates present across the vineyard, S2 was placed in the Grenache which is approximately 30 meters higher in elevation than S1 and S2 and located on a steeper slope. Lastly, the vineyard operations extend to a site on the Clearwater River, approximately 2 kilometers away on a Southeast facing slope. The vineyard manager has observed differences in plant growth here compared to the North vineyards, so S4 was placed in the Syrah to quantify the observed differences in climate.

Figure 3.3: Vineyard weather station field set up (S4, Syrah)

Vineyard operations and accessibility had to be considered for the station placement within the blocks. For example, row spacing was narrower in the Syrah, so S4 had to be placed at a row end such that a tractor mounted with a boom could maneuver around the station. Data on near-canopy weather, canopy spectral reflectance, and soil moisture characteristics were collected on 5-minute intervals from May 1st to September 13th, 2019 for a total of 135 days of data. The Arduino based data loggers described in Chapter 1 were used for data collection. Parameters measured at each station and their associated configuration are described in Table 3.1, and the station set up is shown in Figure 3.3 above.

Table 3.1: Station details and sensor configuration

Station ID	Variety	Parameter (sensor height)
S1	Chardonnay	ATMOS 41(2.24 m) Soil moisture (-0.075 m) Soil matric potential (-0.075 m) Leaf wetness (2.12 m) Canopy temperature (2.17 m) Canopy spectral reflectance (2.14 m)
S2	Grenache	ATMOS 41 (2.19 m) Soil moisture (-0.075 m) Soil matric potential (-0.075 m) Leaf wetness (1.73 m) Canopy temperature (2.03 m) Canopy spectral reflectance (2.12 m)
S3	Riesling	ATMOS 41 (2.05 m) Soil moisture (-0.075 m) Soil matric potential (-0.075 m) Leaf wetness (1.60 m) Canopy temperature (1.70 m) Canopy spectral reflectance (1.80 m)
S4	Syrah	ATMOS 41 (2.18 m) Soil moisture (-0.075 m) Soil matric potential (-0.075 m) Leaf wetness (1.98 m) Canopy temperature (2.11 m)

Vineyard Canopy Surveys

Surveys were conducted every two to three weeks, for a total of 9 surveys in the 2019 growing season (5/12, 5/29, 6/13, 6/25, 7/19, 8/05, 8/23 and 9/13). Because there was very little canopy and leaf area during May surveys, these surveys were omitted from analysis because data was not representative of near canopy conditions. Three rows surrounding each weather station were surveyed to measure near canopy air temperature, relative humidity, canopy temperature, and plant hyperspectral radiance, see Figure 3.4. Between 15 and 25 plants were measured in each row, for a total of about 240 plants sampled in each survey, see Table 3.2 for exact number of plant samples. In addition to the nine surveys at Colter's Creek (CCV), an additional survey was conducted at a nearby vineyard that had an active Powdery Mildew infection, this site is denoted VIN. A total of six rows were surveyed at VIN, two rows of Riesling impacted by PM, and four rows of Chardonnay severely impacted by PM. Upon request, no geo-rectified maps of VIN will be shown for their privacy of the vineyard owners.

Row ID	Variety (Site)	# plants
27	Riesling (CCV)	18
28	Riesling (CCV)	17
29	Riesling (CCV)	18
9	Chardonnay (CCV)	15
10	Chardonnay (CCV)	16
11	Chardonnay (CCV)	16
47	Grenache (CCV)	25
48	Grenache (CCV)	25
49	Grenache (CCV)	25
39	Syrah (CCV)	20
40	Syrah (CCV)	20
41	Syrah (CCV)	20
1	Riesling (VIN)	26
2	Riesling (VIN)	27
3	Chardonnay (VIN)	36
4	Chardonnay (VIN)	36
5	Chardonnay (VIN)	36
6	Chardonnay (VIN)	36

Table 3.2: Description of samples for surveyed rows

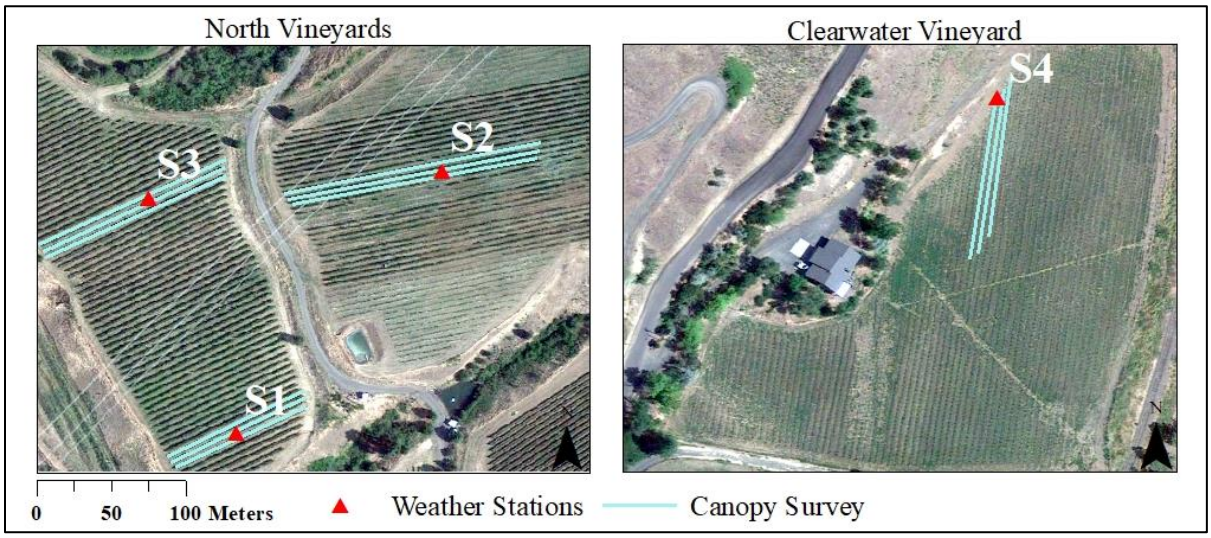

Figure 3.4: Map of surveyed rows (Julieata, ID)

The survey rod set up is shown in Figure 3.5. To measure the near canopy microclimate, a Sensiron SHT-31 temperature and humidity sensor was mounted inside a custom radiation shield. An Apogee SIF-411 Infrared thermometer measured canopy apparent temperature, and an Apogee SP-421 Silicon-cell pyranometer measured incoming solar radiation. The Apogee SS-120 field spectroradiometer was used to measure the energy flux density of the canopy radiation in thw wavelength range of 635nm to 1100nm. The spectroradiometer was mounted at an approximate height of 1.5 meters, pointed downward at a 45° angle from the vertical toward the canopy. The spectral measurement was triggered manually using Apogee software, and an Arduino datalogger queried the other sensors every 10 seconds. A Ubox GPS was also attached to the rod and sampled every second to obtain a geolocation for each plant surveyed.

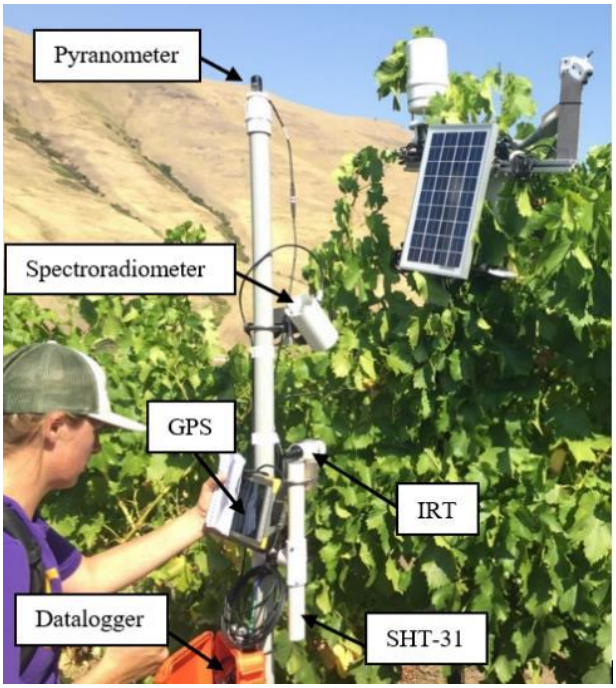

Figure 3.5: Survey rod sensor configuration

Analytical Methods

Gap Filling

As the case with environmental studies, there were some periods of missing data. A combined linear regressing equation was used to fill the gaps in the data. Linear regression was used to develop regression equations between each station for every weather parameter. When one station was not operating, a combined regression equation from the other running stations was applied to estimate the missing data, Equation 3. The R-square value for each regression equation was used to weight the contribution of the weather data. For example, if S1 was not operating, and m_i is the slope, b_i is the

intercept and R_i is the R-square value form the regression equation between S1 and the other operating stations (i = S2, S3, S4) in the form of:

$$Y = mX + b$$

$$T_i = m_i * T_{S1} + b_i$$

Solving for the unknown independent variable:

$$T_{s1} = \frac{T_i - b_i}{m_i}$$

Then the applied regression equation to fill the missing air temperature data for S1 (T_{S1}) from S2, S3 and S4 data is as follows:

Equation 3: Weather data gap filling

$$T_{S1} = \left(\frac{1}{R_{S2} + R_{S3} + R_{S4}}\right) * \left[\left(R_{S2} * \frac{T_{S2} - b_{S2}}{m_{S2}}\right) + \left(R_{S3} * \frac{T_{S3} - b_{S3}}{m_{S3}}\right) + \left(R_{S4} * \frac{T_{S4} - b_{S4}}{m_{S4}}\right)\right]$$

Hereinafter, any data product that uses a cumulative function, including the daily PMRI value, cumulative growing degree days, and cumulative reference ET are calculated with the gap filled data. Comparisons between weather distributions only use the raw data with the gaps left unfilled.

Powdery Mildew Risk Index Calculation

The station air temperature data were used to calculate the UC Davis IPM Powdery Mildew Risk Index (PMRI). The UC Davis Powdery Mildew Risk Assessment Index (PMRI) is the most widely accepted tool to inform pesticide application in vineyards in California. The PMRI is a weather based index used to estimate the growth rate of powdery mildew and provide an indicator of disease pressure (Gubler et al., 1999). It identifies the risk of primary infection from spores based on leaf wetness duration and ideal temperature conditions. Once the initial infection is established, the secondary phase of the PMRI is used to assess pathogen risk severity throughout the season based solely on air temperature. The PMRI ranges from 0 – 100 and points are added and subtracted based on a temperature threshold (Gubler et al., 1999). When the temperature is between 70 – 85°F, conditions are favorable for powdery mildew growth, and temperatures above 95 are harmful to the fungus. The daily value of the index provides growers with a severity level for disease pressure (high, moderate, or low) that is associated with a recommended fungicide spray interval.

The PMRI was calculated by smoothing the 5-minute data into a 6-hour running average using convolution. The primary infection began when three consecutive days had at least one 6-hour period

of favorable temperatures, and the daily index was set to 60 points. Hereinafter, twenty points were added to the daily index if there was at least one 6-hour period that always within the favorable temperature range. If a day did not contain a 6-hour period within the favorable temperature range, or if temperatures exceeded 95°F for at least fifteen minutes, ten points were subtracted from the index. Figure 3.6 shows a description of the conditional statements and associated PMRI adjustments.

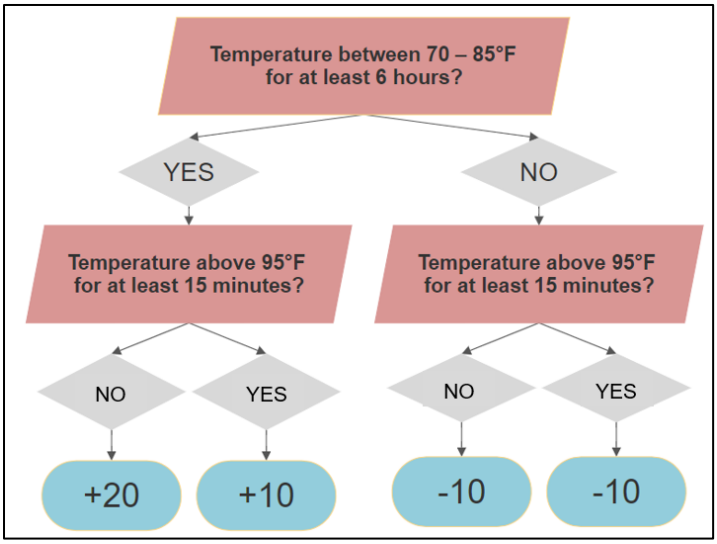

Figure 3.6: Conditional statements associated with adjustment to daily PMRI value

Growing Degree Days Calculation

Growing degree days (GDD) are a measure of heat accumulation above a minimum temperature, or a base temperature, that can inform development stages of crops, disease or insects. GDDs were calculated for each station to show relative differences in growth conditions across the vineyard. The cumulative GDD across a season are often used to inform planting and harvesting dates, or disease life cycles. Standard GDD calculators begin on April 1st. This study collected data from May 1st to September 13th, and so the GDD values only show relative differences between stations, and not absolute cumulative values. The AgriMet GDD equation was used, where the minimum and maximum daily temperatures are used to obtain a daily mean temperature, and 10°C is used as the base temperature.

Equation 4: AgriMet Growing Degree Day

$$GDD = \frac{(Tmin + Tmax)}{\mathbf{2}} - 10°C$$

Reference ET calculation

The Penman-Monteith method was used to calculate daily reference evapotranspiration using an alfalfa reference for each station ("ASCE Manual 70 – Second Edition," 2015). Potential ET is a measure of the weather-related crop water use over a well-watered alfalfa crop. It is not a measure of actual crop evapotranspiration, and so it does not characterize the crop water demand related to soil moisture content, varietal differences, or crop development. To obtain a more accurate estimate of crop ET, a calibrated crop coefficient for grape vines would need to be applied to the reference ET. Further, for direct measurement of actual ET, a more sophisticated method would need to be employed such as use of sap flow sensors or eddy covariance. The equation used to calculate the standardized reference ET for alfalfa reference (ET_{rs}) is as follows:

Equation 5: P-M Reference Evapotranspiration

$$\lambda ET_{rs} = \frac{0.408\Delta(R_n - G) + \gamma * \left(\frac{C_n}{T + 273}\right) * u_2(e_s - e_a)}{\Delta + \gamma(1 + C_d u_2)}$$

Where Δ is the slope of the saturation vapor pressure curve, γ is the psychometric constant, e_s is the saturation vapor pressure, e_a is the actual vapor pressure, R_n is the net radiation, G is the ground flux density, u_2 is the horizontal wind speed measured at 2 meters, and T is the air temperature in degrees Celsius. For the alfalfa reference on a daily time step C_n = 1600 and C_d = 0.38. The calculations for all terms can be found in Appendix A.

Survey Data Processing

The environmental data collected during the vineyard surveys were combined with the GPS data by interpolating the timestamps. The survey data collected 10 second intervals were interpolated to match the GPS data timestamps, which were collected on 1s intervals. Because the environmental data was collected continuously, the IRT captured more than just canopy conditions. For example, the IRT often captured the sky or soil temperature while the survey rod was being maneuvered. Additionally, the time response of the IRT created a lag in the data when the sensor was moving. To mitigate these two falsities in the data, the first derivative of temperature with respect to time was used as a filter. If the temperature derivative exceeded 0.10°C/sec, the sample was considered a transition period and removed. This ensured that only the data collected when the rod was not in motion, i.e. facing a plant, was considered.

Stress Index Calculation

To assess the spatial distribution of plant stress, climate data collected from the canopy survey have been transformed into a weather-related stress index. The index combines the near canopy vapor pressure deficit and leaf temperature depression to show the plant's response to the atmospheric demand for evaporation. The vapor pressure deficit (VPD) is the difference between the saturation vapor pressure(e_s) of the air and the actual vapor pressure (e_a) of the air:

$$VPD = e_s - e_a$$

The saturation vapor pressure varies with temperature and describes the maximum pressure of water vapor in a saturated parcel of air. The higher the air temperature, the more vapor the air can hold, and consequently the higher the saturation vapor pressure.

$$e_s = 0.6018 \exp\left(\frac{17.27T}{T+237.3}\right)$$

The actual vapor pressure is a measurement of the water vapor concentration in the air, and can be calculated from a measurement of relative humidity:

$$e_a = \frac{\%RH}{e_s} * 100$$

VPD is a major driver of potential evapotranspiration and describes the drying power of air. A large VPD will result in an increased demand for water from the land and vegetation to the atmosphere. Conversely, a low VPD results in lower potential evapotranspiration because the atmosphere has less ability to accept water vapor, and stifles evaporative fluxes.

Actual crop evapotranspiration is difficult to measure directly, and so the leaf temperature depression (LTD) can be used to approximate plant transpiration. The LTD is the difference between the air temperature and the apparent canopy temperature, measured using an infrared thermometer.

$$LTD = T_{canopy} - T_{air}$$

When the plant is transpiring, the canopy temperature will be cooler than the ambient air because of evaporative cooling, and the LTD will be more negative. Conversely, when there is less transpiration, the leaf temperature will be closer to the air temperature, and the LTD will be smaller, or less negative. Although the LTD and VPD are interrelated, as they are both function of air temperature, they provide unique information. The VPD provides information on the atmospheric demand driving ET and the LTD provides information on the plant's response to its environment, including atmospheric, soil-water, and physiological conditions. An index was developed to combine LTD and

VPD information into a single unitless value. This index is used to characterize how plant transpiration responds to the environment and show patterns of plant stress in time and space. Physically, it is assumed that a plant exhibiting limited transpiration under conditions of large VPD is experiencing weather related stress.

The leaf temperature depression data from the entire season were normalized using Equation 6, denoted LTD_{Norm}. The data were normalized over the entire dataset because we want to compare relative differences across the entire season, and not just differences in a given survey. The bounds of the normalized data are between 0 and 1, where the lower values represent a small LTD (leaves closer to air temperature) and larger values represent a large LTD (cooler leaves). The vapor pressure deficit data from the entire season were normalized using Equation 7, denoted VPD_{Norm}. Here, small values represent more saturated air and high values represent more capacity for water to evaporate.

Equation 6: Leaf temperature depression normalization

$$LTD_{Norm,i} = \frac{\max(LTD) - LTD_i}{\max(LTD) - \min(LTD)} \; ; \; 0 \leq \; LTD_{Norm,i} < 1$$

Equation 7: Vapor pressure deficit normalization

$$VPD_{Norm,i} = \frac{VPD_i}{\max(VPD)}; \quad 0 < \; VPD_{Norm,i} < \; 1$$

These two normalized values were combined into an index which informs how plant transpiration responds given the local atmospheric demand, Equation 8. Low values of the stress index indicate a plant that is showing signs of stress given the atmospheric demand, and large values indicate a plant that is freely transpiring given the atmospheric demand. For example, if the plant is showing signs of low transpiration (small LTD_{Norm}), but the atmospheric demand for water is low (low VPD_{Norm}), we would identify this plant as less stressed (greater DD_{Index}). Conversely, if a plant was showing signs of low transpiration, but the atmospheric demand for water was high, then we would identify this plant as exhibiting stress (lower DD_{Index}).

Equation 8: DD Stress index

$$DD_i = \frac{LTD_{Norm,i}}{VPD_{Norm,i}}; \quad 0 \leq \; DD_i < \; \infty$$

Statistical Procedure to Identify Outliers

A statistical test was created to identify plants that do not conform to the expected DD index value, or expected level of stress, for a given variety and time of year. To do this, the DD index was calculated for both the continuous station data and the data from the six canopy surveys. The vertical purple

lines in Figure 3.7 show the range of values measured during a given hour for the month of June. The average DD index for a given time of day in each month was calculated for the four stations, shown as the blue line in Figure 3.7. For example, this provides the average DD index observed at Station 1 at 10:00 AM in June and quantifies the typical response of the plant during this time of day and during this time of the season. The data from the plant surveys were then compared to this typical value, based on the time of day and the month the survey was conducted, shown as the red data points in Figure 3.7. If the DD index from the survey data deviated from the typical response by more than two standard deviations, it was deemed significant.

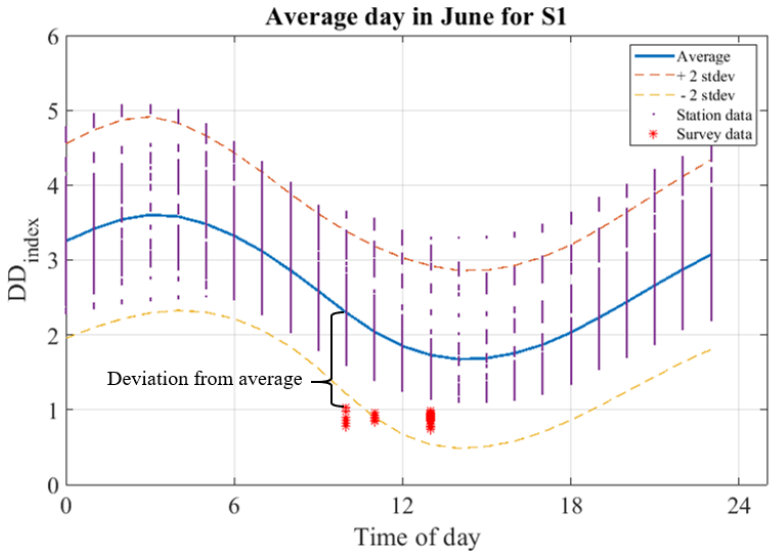

Figure 3.7: Visualization of procedure used to identify individual plants exhibiting stressed behavior

Hyperspectral Data Processing

The Apogee SS-120 field spectroradiometer SS-120 reports the energy flux density of the canopy in units of counts. A white reference was not used to measure the spectrum of incoming radiation from the sun. Because of this, the hyperspectral signatures are not reported in terms of reflectance of incoming light, but rather as plant photon density. A white reference is used to control for variables which affect spectral irradiance at the Earth's surface including solar aspect and elevation, atmospheric absorption, air water vapor concentration, and aerosol loading. To control for some of these variables, the measurements were taken at approximately the same time of day for each survey, and surveys were only conducted on days with limited cloud cover. To account for the inherent sensor noise, the dark noise value (3 counts) was subtracted from the raw counts at each wavelength.

The spectroradiometer reports measurements at a 1 nm resolution, though the spectral resolution of the sensor given it's full-width half max specification is 3nm. To ensure that the hyperspectral measurements represent the sensitivity of the sensor, convolution was used to calculate a running

average of the radiance values over a 3nm centered window. The data were then normalized by the maximum count value of each signature. This was done to control for the variability in the measurement intensity due to changes in incident radiation. Vegetation indices that related to plant disease incidence, plant water status and plant development were found from literature. Table 3.3 describes the calculated indices used in this assessment. Most of the VIs used were specified for use with grapevines (V. *vinifera*), though some are generalized to a variety of plant species including the chlorophyll red edge and water index.

Table 3.3: Vegetation indices descriptions

Vegetation index	Description	Equation	Citation
Water index	Describes the plant water content, where a small value represents less water content.	$WI = \frac{\rho_{970}}{\rho_{900}}$	(Peñuelas et al., 1993)
Chlorophyll red edge	Describe the chlorophyll content, is also an indicator or disease development	$CRE = \frac{\rho_{780}}{\rho_{710}} - 1$	(Gitelson et al., 2006)
Hyperspectral normalized difference vegetation index	Describes plant green-ness and is correlated with LAI and plant development.	$hNDVI = \frac{\rho_{814} - \rho_{672}}{\rho_{814} + \rho_{672}}$	(Gamon et al., 1992; Oppelt & Mauser, 2004)
Veraison band ratio	Describes the photosynthetic activity by comparing the red edge to near infrared reflectance.	$verBR = \frac{\rho_{648}}{\rho_{715}}$	(Ozelkan et al., 2015)

Statistical Analysis

Air temperature, relative humidity, and wind speed are parameters that are known to influence the development and spread of powdery mildew. To assess the variability in weather across the vineyard, the two sample Kolmogorov-Smirnov (K-S) test was used to check for significant difference between the distributions of these weather parameters observed at each station. The K-S test is a common statistical procedure used in climate and meteorological sciences (Hennemuth et al., 2013). The two sample K-S test compares one empirical distribution to another empirical distribution to determine if the two distributions are significantly different. A distribution with a cumulative density function $F(x)$, is compared to a second distribution with a cumulative density function $G(x)$ using the following hypothesis test:

$$H_0: F(x) = G(x); \qquad H_1: F(x) \neq G(x)$$

The K-S test was used in this study because it makes no underlying assumption of the distribution of the data, unlike other common statistical tests such as Chi Squared or Student's T-test which assume normally distributed data. This is an important distinction when working with weather data is often skewed and does not conform to the definition of a Gaussian distribution(Quevedo & Gonzalez,

2017). For example, the mean and standard deviation between two nearby air temperature measurements are likely to be the same, but the distributions might differ significantly at specific temperatures ranges. These differences are not captured in the student's t-test but are the basis for the K-S test statistic. The test statistic, D, is given by the maximum absolute difference between the two distributions to determine if they are significantly different. See Equation 9 and Equation 10 for the test statistic and associated significance criteria, where n and m are the number of samples in F and G, respectively.

Equation 9: Kolmogorov-Smirnov test statistic

$$D = \max\left(|F(x) - G(x)|\right)$$

Equation 10: Kolmogorov-Smirnov significance criteria

$$D > K_\alpha \sqrt{\frac{n+m}{n*m}}; \quad K_{\alpha=0.05} = 1.36$$

A one-way analysis of variance was used to test for significance between the differences in hyperspectral vegetation indices. First, ANOVA was used to test for significant differences in vegetation indices over time for varieties at Colter's creek vineyard. This is to test if field-based methods of hyperspectral remote sensing can be used to distinguish developmental differences in the plants. Secondly, ANOVA was used to test for significant differences between diseased and healthy plants. Because measurements of the diseased group were taken at a different time, and at a different vineyard than measurements of the healthy plants, it is necessary to control for variation in the groups related to development stage. The one-way ANOVA tests the null hypothesis (H_0) that the calculated vegetation indices from samples taken on different dates are drawn from populations with the same means ($\overline{VI}_{date}$) against the alternative hypothesis (H_1) that the samples are drawn from populations with unequal means.

$$H_0: \overline{VI}_{6/12} = \overline{VI}_{6/25} = \overline{VI}_{7/19} = \overline{VI}_{8/05} = \overline{VI}_{8/23} = \overline{VI}_{9/13}$$

$$H_1: \overline{VI}_{6/12} \neq \overline{VI}_{6/25} \neq \overline{VI}_{7/19} \neq \overline{VI}_{8/05} \neq \overline{VI}_{8/23} \neq \overline{VI}_{9/13}$$

Similarly, for testing for significant differences in vegetation indices for diseased and healthy leaves, the hypotheses test are as follows:

$$H_0: \overline{VI}_{healthy,8/05} = \overline{VI}_{Diseased,\ 8/08}$$

$$H_1: \overline{VI}_{healthy,8/05} \neq \overline{VI}_{Diseased,\ 8/08}$$

Results

Observed Differences in Microclimates

This section will compare the microclimates observed at each weather station. The results from the two sample K-S test show that there are significant differences in the four weather parameters that are influential to powdery mildew growth: temperature, relative humidity, and wind speed. In general, differences between the stations were greatest in the early part of the season, from May 1st – June 30th. After July, the four stations become similar in their temperature, relative humidity, and wind speed distributions.

Air Temperature

First, the daytime temperature distribution varied significantly between all stations in the early season. Most notably were differences observed between S4 in the Syrah and S2 in the Grenache. S4 had significantly warmer daytime temperatures than the other three stations, see Figure 3.8A. The range of S4 in the early part of the season shows that the minimum temperature experienced in the Syrah was more than 5°C greater than the other three stations. S2 was generally cooler than S1 and S3. These trends did not persist into the later part of the season (July – September), as seen in Figure 3.8B. After July, all stations appeared to have very similar temperature distributions.

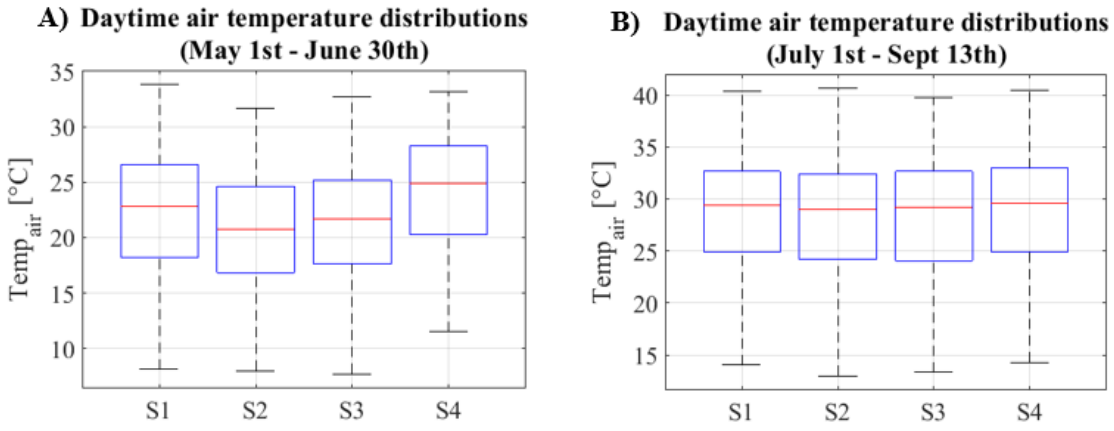

Figure 3.8: Daytime air temperature distributions for early season (May 1 – June 30th) and late season (July 1st – Sep. 13th)

Table 3.4 shows the p-values from the K-S significance test between each station for four subsets of the data; early season daytime, early season nighttime, late season daytime and late season nighttime. Significant differences are shown in bold text. All combinations were found to have significant different c.d.f.s, except for the nighttime temperatures between S1 and S2 in the later part of the season.

Table 3.4: P-values from two-sample KS test for air temperature c.d.f.s (95% confidence)

	S1 vs S2	S1 vs S3	S1 vs S4	S2 vs S3	S2 vs S4	S3 vs S4
Temp day (Early Season)	**2.2E-42**	**8.86E-23**	**2.93E-56**	**4.92E-9**	**2.2E-139**	**2.2 E-125**
Temp night (Early Season)	**2.7E-13**	**1.4E-18**	**4.07E-23**	**0.032**	**2.3E-48**	**4.1 E-63**
Temp day (Late Season)	**0.0018**	**0.0048**	**8.7E-4**	**0.043**	**2.8E-7**	**1.2 E-6**
Temp night (Late Season)	0.22	**0.0081**	**1.7E-11**	**0.018**	**2.5E-09**	**5.6 E-7**

Relative Humidity

Second, the differences in relative humidity distributions experienced at each station were greatest in the early part of the season (May – June), Figure 3.9A. Most significant were differences between S4 and the other three stations, where S4 rarely exceeded 83% relative humidity. S1 also differed slightly from the S3 and S2, with fewer samples above 90% RH. This is surprising given the proximity between S1 and S3. Like air temperature, the distributions become very similar after July, Figure 3.9B. All combinations were found to have significantly different c.d.f.s except for daytime relative humidity between S2 and S3 in the late season, and nighttime relative humidity between S1 and S2 in the late season, see Table 3.5.

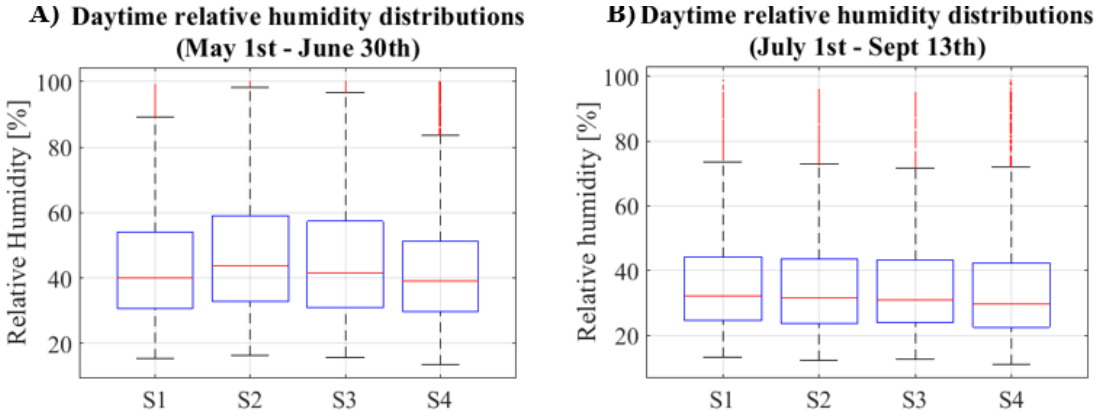

Figure 3.9: Daytime RH distributions for early season (May 1 – June 30th) and late season (July 1st – Sep. 13th)

Table 3.5: P-values from two-sample KS test for relative humidity c.d.f.s (95% confidence)

	S1 vs S2	S1 vs S3	S1 vs S4	S2 vs S3	S2 vs S4	S3 vs S4
RH day (Early Season)	**3.4E-18**	**4.4E-07**	**0.00049**	**1.9E-5**	**1.2E-26**	**7.8E-13**
RH night (Early Season)	**6.9E-7**	**1.9 E-12**	**4.0 E-61**	**0.0032**	**2.9E-37**	**5.1E-38**
RH day (Late Season)	**0.0038**	**0.015**	**1.2 E-15**	0.4s	**2.2E-6**	**8.1E-7**
RH night (Late Season)	0.15	**3.2E-08**	**2.6E-16**	**9.5E-5**	**1.8 E-21**	**1.5E-36**

Wind Speed

Figure 3.10 shows the differences in daytime wind speed distributions for the early season and late season. The boxplots were constrained to only show wind speeds below 5m/s because there were some large outliers that skewed the y-axis scale. The general trends show that wind speeds were much greater during the early part of the season (May – June) than the later season. Station to station comparison show that S2 generally saw higher wind speeds than the other three stations, and S4 at the Clearwater vineyard consistently had lower wind speeds than the north vineyards, see Figure 3.10A. Differences prevailed throughout the later part of the season, though they were not as significant, Figure 3.10B. Table 3.6 show results from the two-sample K-S test. All the combinations were deemed significant.

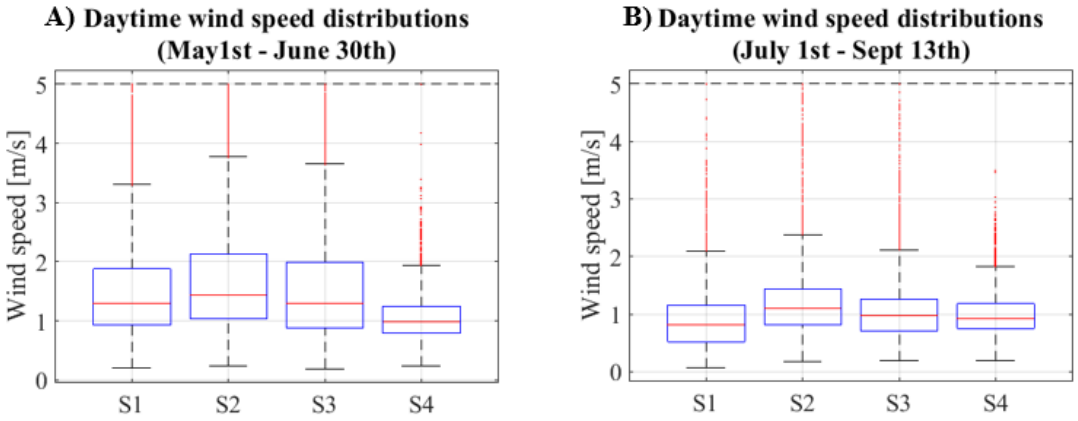

Figure 3.10: Daytime wind speed distribution for early season (May 1 – June 30th) and late season (July 1st – Sep. 13th)

Table 3.6: P-values from two-sample KS test for wind speed c.d.f.s (95% confidence)

	S1 vs S2	S1 vs S3	S1 vs S4	S2 vs S3	S2 vs S4	S3 vs S4
Wind speed day (Early season)	**3.1E-21**	**0.0031**	**1.08E-180**	**1.5E-22**	**1.9E-264**	**3E-168**
Wind speed night (Early season)	**7.8E-98**	**0.011**	**0**	**8.8E-104**	**0**	**0**
Wind speed day (Late season)	**4.4E-133**	**1.5E-42**	**1.2E-107**	**1.9E-26**	**4.5E-77**	**3.8E-10**
Wind speed night (Late season)	**0**	**0**	**3.2E-168**	**2.45E-135**	**0**	**0**

Calculated Meteorological Metrics

General trends show that there are statistical differences in the distributions of air temperature, relative humidity, and wind speed across the four locations. However, plants are not concerned with statistician differences, and p-values do not inform on-farm management decisions. More sophisticated data products are needed to infer differences in plant physiologic responses. This section will show comparison of the calculated variables between stations including the Powdery Mildew Risk Index (PMRI), Growing Degree Days, and Penman Monteith reference Evapotranspiration.

Powdery Mildew Risk Index

The daily PMRI values for each station are shown in Figure 3.11. Red, black and green horizontal lines indicate thresholds for the recommended spray regime. For example, for sulfur fungicides, a weekly spray application is recommended for PMRI values above 60, a bi-weekly application is recommended for values between 40 and 60, and a 21-day application is recommended for values below 30. Results show the PMRI changed substantially over the course of the growing season and across the different locations. In general, the highest disease pressure occurred in early May and again in June through July. All stations fell below the high disease pressure threshold through-out August. When looking at difference between stations, most notable was S4, which generally had a lower disease pressure than the other three stations for the entire growing season. S3 and S2 generally had the highest disease pressure across the entire season. Surprisingly, S1 deviated substantially from S3 in June, despite their proximity.

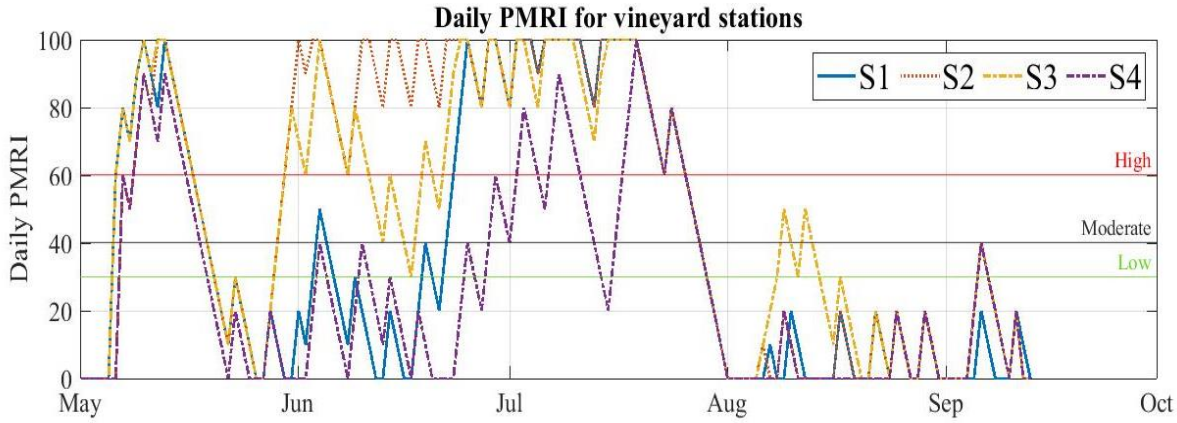

Figure 3.11: Daily PMRI values over the growing season for each station. Green, black and red horizontal lines represent the disease pressure severity levels and are associated with different recommended spray regimes

Growing Degree Days

The cumulative GDD for the season is shown in Figure 3.12. This plot shows that there are minimal differences in the GDD accumulation between the four stations during the study period. The greatest difference is seen at S4, which was about 75-100 units higher than the other three stations. This is consistent with the farmer's observations that the Clearwater site is often a week or two ahead of the other stations and is consequently harvested earlier.

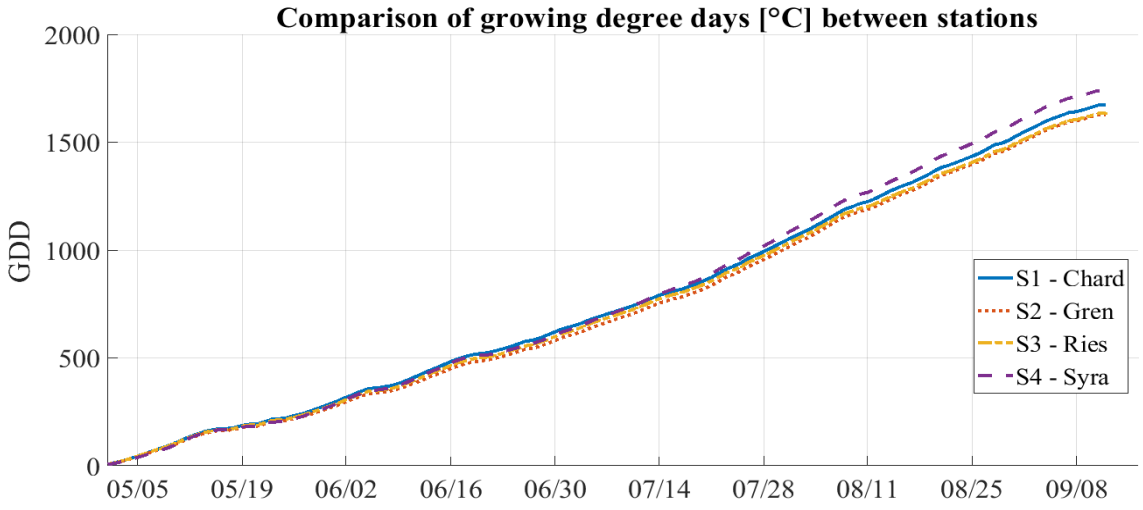

Figure 3.12: Cumulative GDD (May 1st – September 13th, 2019)

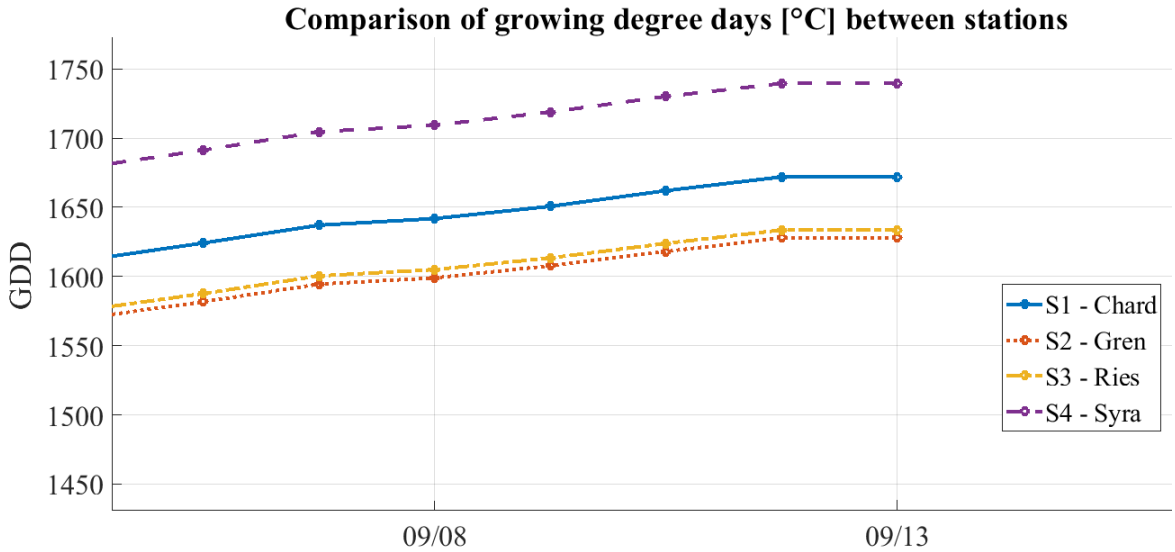

Figure 3.13: Comparison of cumulative GDD value at the end of season

Reference ET

The daily reference ET in millimeters for each station are shown in Figure 3.14. This does not show variation in actual ET between varieties, but rather the weather-related crop water demand. In general, the daily values are very similar from May through June. This shows that the weather-related crop water use does not vary substantially across the vineyards in the early part of the season. Beginning in late-July, the daily reference ET starts to vary more substantially between stations, as much as a millimeter or two on some days. This is the opposite trend observed when just looking at the raw weather date distributions in the previous section.

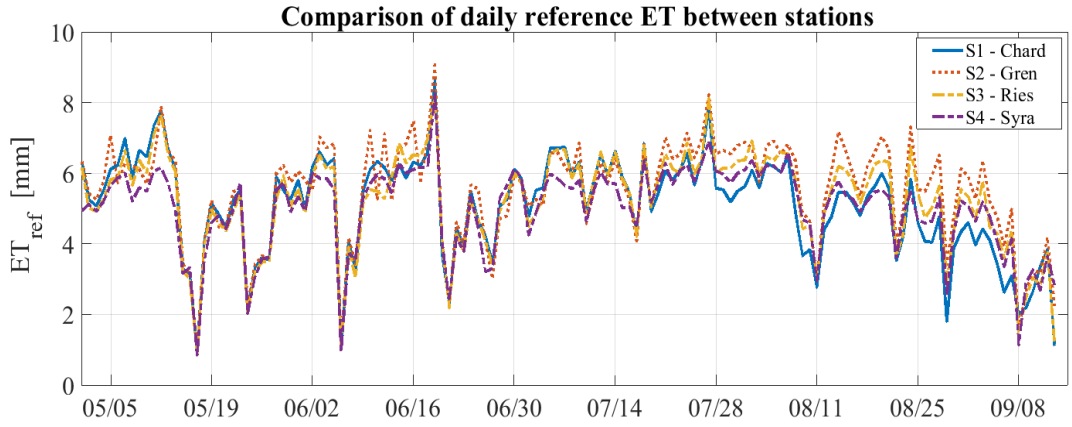

Figure 3.14: Daily reference ET (May 1st – September 13th , 2019)

These small daily differences are magnified when looking at cumulative reference ET, representing the total crop water demand driven by local weather over the entire season in units of millimeters. Figure 3.15 shows the differences in cumulative reference ET between the stations, and Figure 3.16 more clearly shows the values at the end of the season. This shows that the total water demand at S2 in the Grenache is approximately 75mm, roughly 3 inches, more than the water demand at S4 in the Syrah.

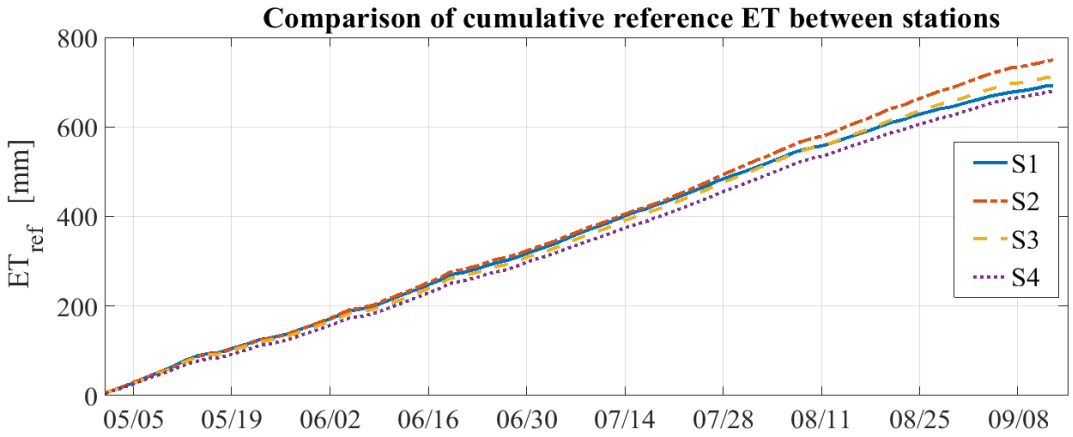

Figure 3.15: Cumulative reference ET (May 1st – Septmeber 13th, 2019)

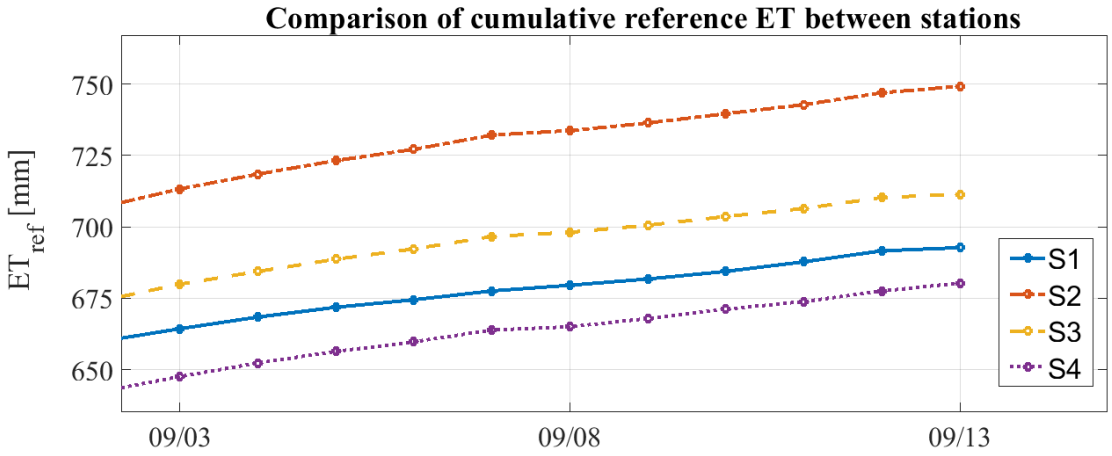

Figure 3.16: Comparison of cumulative reference ET values at the end of season

Spatial variability of canopy characteristics

The previous section compares time varying processes between the four distributed stations. The stations capture weather conditions in the general proximity and describe variability across a field-scale. This section describes the results of the canopy surveys and aims to resolve differences in the near canopy climate to the plant-scale.

Stress Index Maps

The maps below show the spatial variability in the stress index (DD index), such that higher values of the index represent plants freely transpiring given their atmospheric demand, and low values indicate plants with limited transpiration given the atmospheric demand and are exhibiting more stress. Individual samples that were found to be significantly different from the typical values observed at the nearby weather station for that time of day are denoted with a black 'x', refer to Figure 3.7 for this procedure. Figure 3.17 show maps of the stress index in the rows adjacent to the stations for the six surveys through time. The survey on 8/23 is missing Riesling data due to a GPS error, and the survey on 9/13 is missing Chardonnay and Syrah data due to failure of the temperature and humidity sensor.

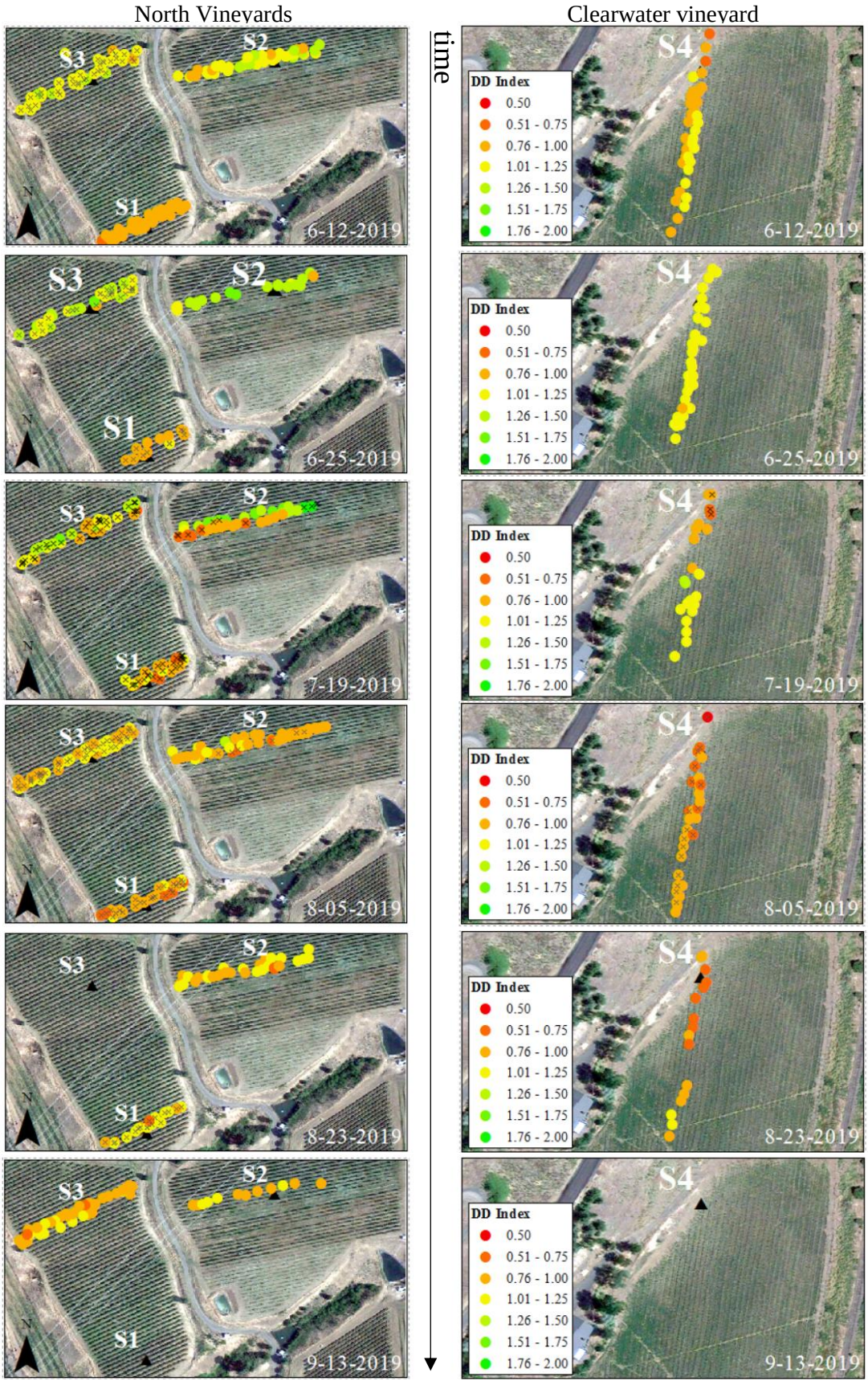

Figure 3.17: Maps of DD Index over time, x denotes values that are significantly different than the nearby station

First, there appears to be a temporal trend, where values across all locations tend to become more stressed as the season goes on, which is to be expected. Also, the earlier surveys on 6/12 and 6/25 had more homogeneity within the varietal groupings, but starting on the 7/19 survey, there was more variability between individual plants within the rows. There were also some clear spatial patterns observed that were persistent throughout all surveys. The Chardonnay (S1) plants were generally more stressed than the Riesling (S3) and Grenache (S2). The Grenache appear to have the least stress near the top of the rows. There do not appear to be any consistent patterns within the Riesling and Chardonnay. The Syrah (S4) at the Clearwater vineyard consistently exhibits the most stress out of all locations. This is consistent with results from the air temperature comparisons, where S4 was significantly hotter and had more GDD accumulation than the rest of the stations. There is also a distinct spatial pattern within the Syrah rows that shows more stress near the end of the rows, closest to the gravel road, though this was not observed on 6/25.

Hyperspectral Indices

The previous sections focus on characterizing the environmental heterogeneity that could lead to difference in disease pressure across the vineyard in space and time. Actual detection of disease is more cumbersome. This section will investigate the ability of field-based methods to detect actual disease presence using a non-imaging spectroradiometer.

Vine Development Stage

First, the ability of hyperspectral vegetation indices (Vis) to distinguish seasonal differences in the varieties is tested. Different groups are represented by the six survey dates, conducted approximately every two weeks. Figure 3.18 shows the two VIs that are associated with plant development, a hyperspectral NDVI index (hNDVI) and a veraison Band Ratio index (verBR) for all varieties. Visually, the verBR was able to better at distinguishing between survey dates compared to the hNDVI. This is validated by the one-way ANOVA results in Table 3.7, which show much smaller p-values for verBR compared to hNDVI in all varieties.

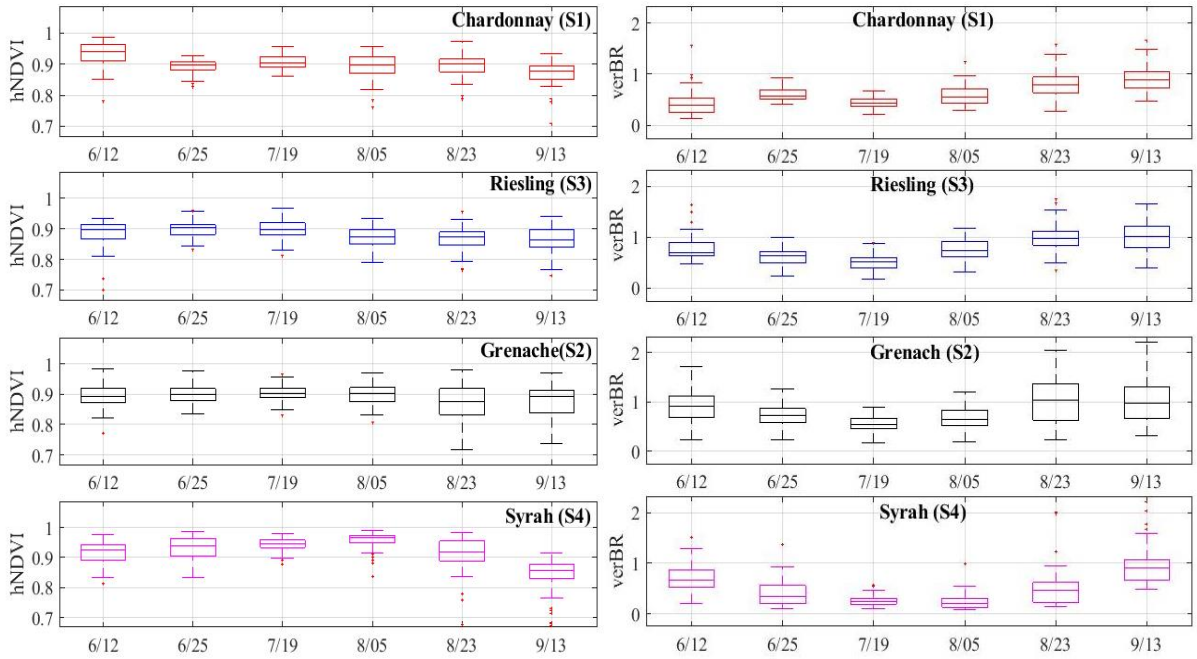

Figure 3.18: Distributions of developmental vegetation indices (hNDVI and verBR) for each survey

Table 3.7: One-way ANOVA p-values comparing the survey means for hNDVI and verBR

	Chardonnay	**Riesling**	**Grenache**	**Syrah**
hNDVI	9.0×10^{-15}*	1.8×10^{-4}*	1.05×10^{-05}*	2.1×10^{-35}*
verBR	2.9×10^{-29}*	8.8×10^{-11}*	1.2×10^{-24}*	1.7×10^{-46}*

*statistically significant (95% confidence)

Secondly, the change in VIs associated with plant disease and water content are compared over time for all varieties. The Chlorophyll Red Edge index (CRE) has been shown to have a negative correlation with disease development, and the Penuelas Water Index (WI_{Pen}) is positively correlated with plant water content. Visually, Figure 3.19 shows that there are clear differences in both VIs between survey dates. For the water index, WI_{Pen}, there is a consistent trend in all varieties. Starting on 6/12 the index increases until it peaks on 7/19, then gradually decreases until 9/13. The trend is especially clear in the red varieties, Grenache and Syrah. There does not appear to be a consistent trend observed for the CRE overtime, but there are stark differences in the range between the different surveys and between varieties. In particular, the variability in the CRE index for Syrah is very large for the 6/25, 7/19, 8/05 and 8/23 surveys.

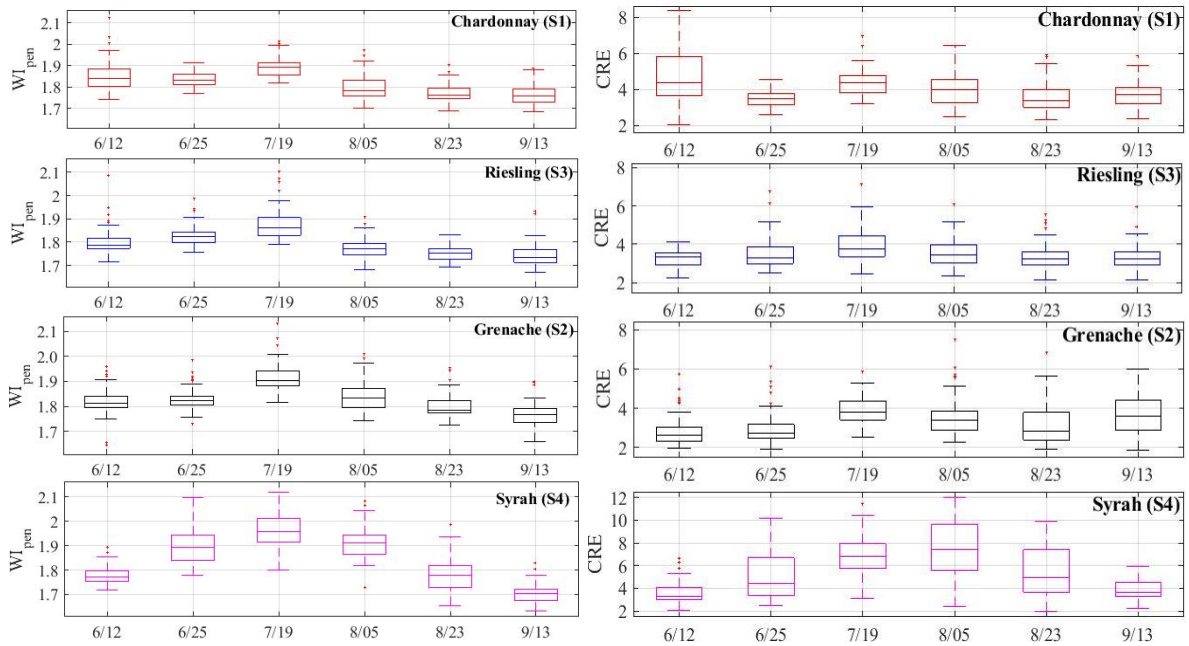

Figure 3.19: Distributions of stress related vegetation indices (WI_{Pen} and CRE) for each survey

Table 3.8: One-way ANOVA p-values comparing the survey means for WIpen and CRE

	Chardonnay	**Riesling**	**Grenache**	**Syrah**
WI_{PEN}	1.6×10^{-33}*	1.7×10^{-48}*	7.6×10^{-44}*	5.8×10^{-91}*
CRE	2.6×10^{-11}*	$7.6 \times 10^{--8}$*	1.02×10^{-15}*	6.4×10^{-33}*

*statistically significant (95% confidence)

Vine Disease Detection

Next, the ability of these VIs to distinguish between plants at the two locations is tested. The two locations are represented by the Colter's Creek Vineyard (CCV) survey conducted on 8/05/2019, and the survey at a different vineyard operation (VIN) conducted on 8/08/2019 which had many plants infected with powdery mildew disease. Figure 3.20 shows a comparison between the two VIs associated with plant development, hNDVI and verBR for Chardonnay and Riesling varieties. A one-way analysis of variance (ANOVA) comparing the group means showed that there was not a significant difference between the group means of plants at CCV and plants at VIN for Riesling varieties, indicating that the plants were at similar stage of development. There was a significant difference for Chardonnay varieties, indicating there might be some variation in the development stage of Chardonnay between the two locations.

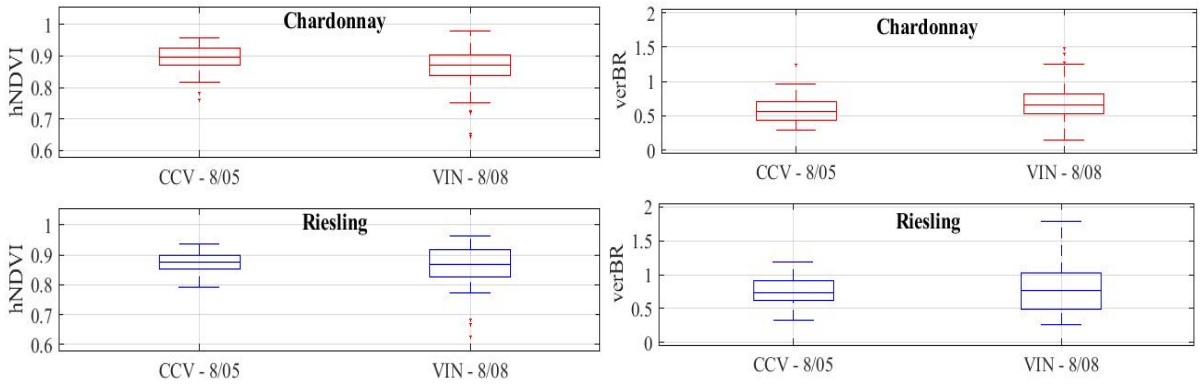

Figure 3.20: Comparison of developmental VIs (hNDVI and verBR) for plants at CCV and VIN locations of Chardonnay and Riesling variety.

Table 3.9: One-way ANOVA p-values comparing the CCV and VIN means for hNDVI and verBR

	Chardonnay	**Riesling**
hNDVI	0.038*	0.654
verBR	0.013*	0.418

*statistically significant (95% confidence)

Next, the Chlorophyll Red Edge index (CRE) and Penuelas water index (WIpen) vegetation indices were compared for the two locations, CCV and VIN, for Chardonnay and Riesling varieties, Figure 3.21. Here, we found that two locations vary significantly in both Riesling and Chardonnay varieties. The CRE was significantly lower at VIN location than CCV. The WIpen was also significantly lower at VIN indicating that Chardonnay and Riesling plants have less plant water content on average at this location.

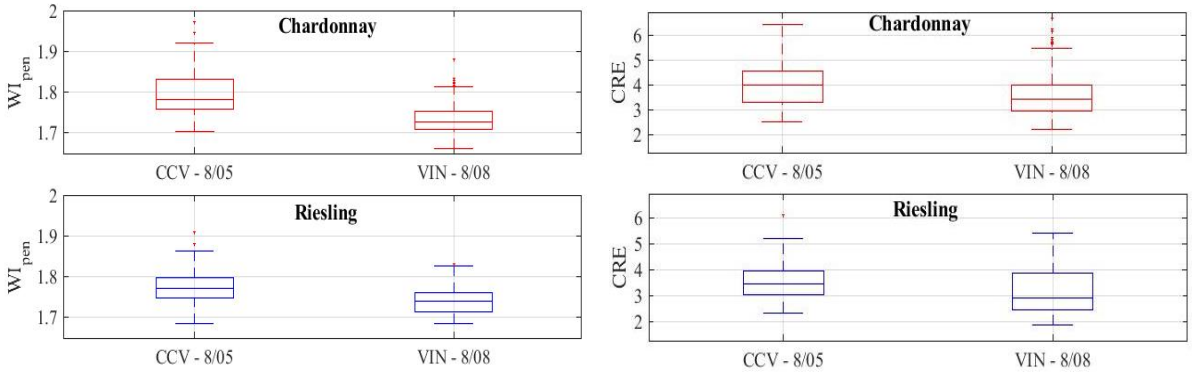

Figure 3.21: Comparison of stress VIs (WIp_{en} and CRE) for plants at CCV and VIN locations of Chardonnay and Riesling variety

Table 3.10: One-way ANOVA p-values comparing the CCV and VIN means for WIpen and CRE

	Chardonnay	**Riesling**
WI_{PEN}	4.8×10^{-21}*	3.1×10^{-7}*
CRE	0.001*	0.009*

*statistically significant (95% confidence)

Discussion

Powdery mildew disease outbreaks in vineyards can be detrimental to production and fruit quality. Farmers need tools to help better inform the timing and location of pesticide applications to mitigate disease and optimize resources management. Unfortunately for our research, but fortuitous for the farmer, powdery mildew disease was not observed in the vineyard this season. Because of this, the weather patterns we observed, and the calculated PMRI cannot be correlated to actual disease establishment. However, results from this study do show variability in the environmental factors that influence disease development, and consequently indicate spatial and temporal variability in disease susceptibility.

The results from this study show that there are at least three distinct microclimates across the vineyard that might have different susceptibility to powdery mildew disease. The distributed weather stations were able to detect significant differences in the distribution of temperature, relative humidity, and wind speed across spatial scales that are pertinent to management decision, *i.e.* across vineyard blocks. These weather parameters are known to influence the development and dispersal of powdery mildew disease. These observations can be put into action by use of the UC Davis Powdery Mildew Risk Index (PMRI). The daily PMRI values calculated at each station vary substantially on a daily basis, as well as over the growing season. This index prescribes a recommended spray regime based on cumulative temperature. As an example, Figure 3.22 compares the recomended spray interval for the Grenache and Syrah vineyard blocks. Data from S4 indicate that a bi-weekly fungicide applciaton is recomended in June, and weekly in July for the Syrah block, but starting in August a three week schedule would suffice. In comparison, a weekly fungicide application schedule is recommended for the S2 block starting as early as June.

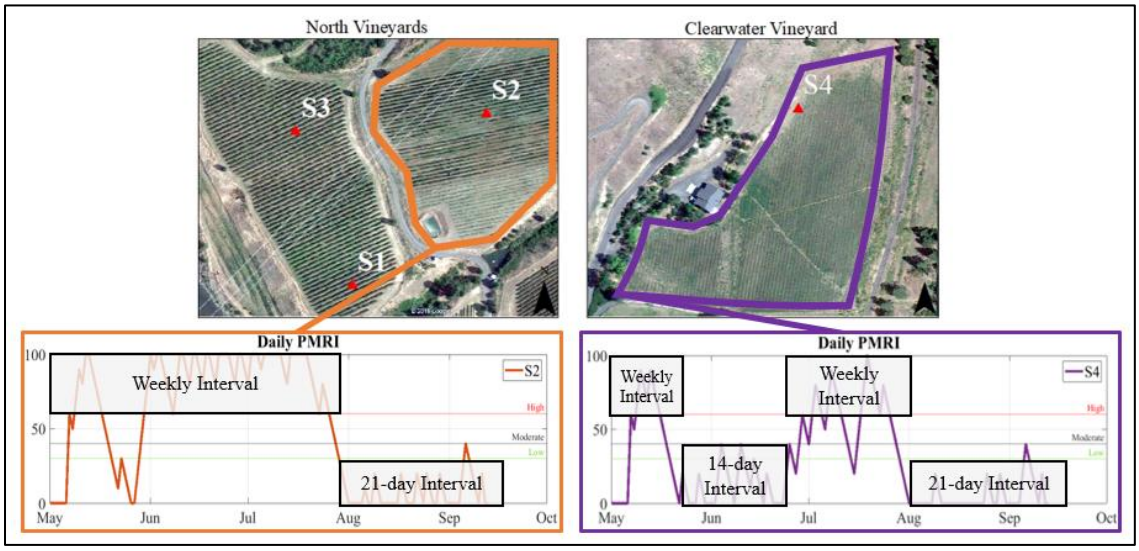

Figure 3.22: Comparison of recommended spray regime for S2 and S4

Although S1 and S3 PMRI values do vary, particularly in June, it might not be feasible to separate this vineyard block into two distinct zones from an operational perspective. In this case, spray regimes for the two blocks shown in Figure 3.23 appear quite similar. However, the difference between four recommended applications and two applications in August could represent savings in labor costs, chemical costs, and environmental damages.

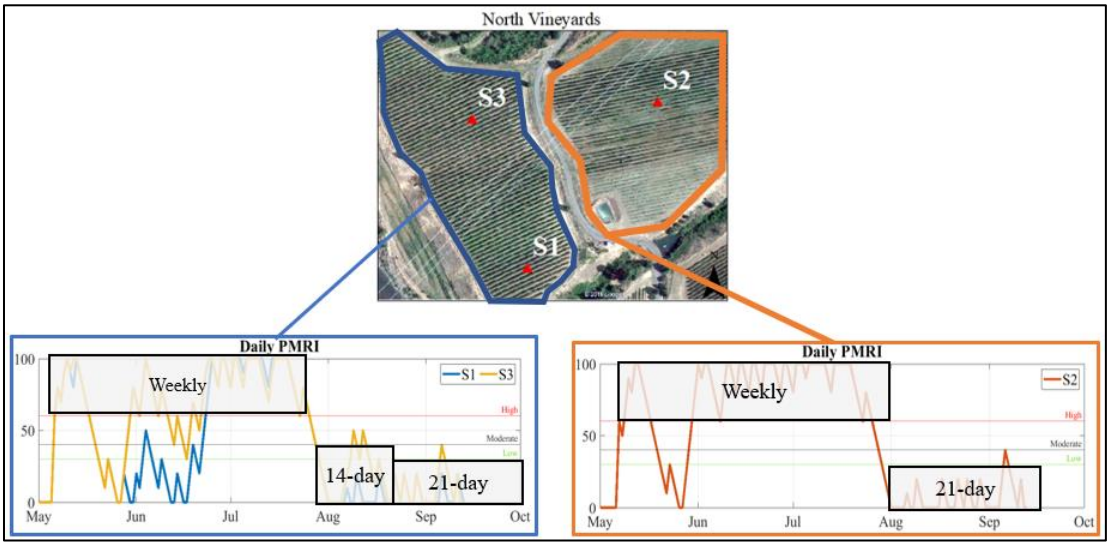

Figure 3.23: Comparison of recommended spray regime for S2 and S1

The spatial patterns of the DD Index observed in the maps (Figure 3.17) indicate that there are detectable differences in plant stress across the vineyard. Most notable were differences between varieties, where Chardonnay and Syrah appeared to be the most stressed, and Grenache showed the least stress symptoms. It was shown that S2 in the Grenache had the greatest reference evapotranspiration, 30 – 75mm more than the other three locations. Despite this, the Grenache plants showed limited stress symptoms in the surveys indicating that the Grenache is a more drought tolerant variety. For this specific vineyard, planting the Grenache in the region with greatest reference evapotranspiration, or weather-related demand for water, was a wise decision. Further, under a water scarce future, Grenache would be a good substitute variety to withstand the hotter and drier conditions anticipated from climate change scenarios.

The clearest spatial trend within rows was observed in the Syrah. Here, it was shown that plants near the end of the rows showed more stress than plants in the middle of the vineyard. This is likely attributed to the increased evaporative demand near the gravel road. From a management perspective, this information could inform irrigation zones such that the row edges are watered more frequently. Results from the stress maps can also be used to investing the spatial variability in disease susceptibility. It has been shown that both over watering and under-watering can contribute to disease

development (Austin & Wilcox, 2011; Stoll et al., 2008; van Niekerk et al., 2011). The Syrah exhibited the greatest stress response throughout the season, possibly exacerbating it's susceptibility to disease, as shown by Stoll et al. (2008) and van Niekerk et al. (2011). Conversely, the PMRI values indicated that Syrah generally had the lowest disease pressure based on hourly air temperature. This highlights the importance of considering multiple environmental factors when designing a pest management plan.

Crop disease detection is a common application of remote sensing technology in agriculture. Many studies have shown robust results for identifying disease in laboratory settings, under ideal light conditions, or with imaging spectroradiometers. This study aimed to assess the ability of non-imaging hyperspectral sensing to detect disease presence on-farm. Because of this, the methods used in this study to collect the hyperspectral data do not conform to typical procedures for spectroradiometer measurements. A white reference was not used to measure the spectrum of incoming solar radiation, and therefore the measurements do not represent a percent reflectance but rather the photon flux density of the canopy. As a result, variables such as solar elevation, solar aspect, and atmospheric absorbance were not controlled for. However, the data collected with relatively simple methods shows that using spectroradiometers on-farm can still be used to monitor plant physiology. Using two vegetation indices correlated with plant development informed by literature, we first showed that the mean values were not equal across all six surveys taken at Colter's Creek over the course of the growing season. Since the surveys were taken approximately two-weeks apart, this indicates that the spectroradiometer was able detect differences in plant development. Similarly, we found that the WI_{Pen} and CRE varied in time.

When comparing the vegetation indices from plants at Colter's Creek to plants at the other vineyard operation, VIN, we found that there was not a significant difference in the developmental indices for Riesling. This indicates that the two plant groups were at similar developmental stages, allowing us to control for this. There was a significant difference for Chardonnay plants, suggesting that the plants might have been at different stages in their development. When comparing the CRE index between the two locations, we found that plants at VIN had significantly lower values of CRE than CCV. Because there was an active powdery mildew outbreak at the VIN location, results of this test indicate that we were able to detect differences between diseased plants and healthy plants. Though because the WI_{Pen} also varied significantly, we cannot rule out that the variance observed in the CRE index is not an artifact of plant water status, and as a result might not be a feature of disease. Though the converse could also be true, in that the diseased plants are at a lower water status because of the disease incidence. For Chardonnay varieties, we cannot rule out the variation observed in the CRE

index is not an artifact of differences in developmental stage between plants at CCV and plants at VIN, and therefore not associated with disease.

In conclusion, this study was able to show temporal and spatial variability of environmental factors that are associated with the development and spread of powdery mildew disease using a relatively low-cost weather stations and field-based hyperspectral sensing. The results of the hyperspectral analysis have laid the groundwork for another vineyard disease detection study planned for the summer of 2020, focusing on Phylloxera. Phylloxera is another devastating disease which is commonly found in Californian vineyards, though it was recently found to be present in a majority of Eastern Washington and Idaho vineyards. This occurrence of Phylloxera is novel in this region, and these preliminary results will provide a baseline for future analyses of disease detection in vineyards. The usefulness of distributed weather stations goes beyond monitoring variability in disease pressure. The stations also showed differences in reference evapotranspiration and growing degree days. These data products could inform other management decisions including irrigation timing, harvesting dates, or frost protection. In conclusion, this study confirmed our hypothesis that there were distinct, significantly different microclimates across the vineyard. As such, the data products provided by these relatively low-cost, on-farm weather stations would benefit farmers. In fact, this information proved useful enough to the vineyard manager that he has expressed interest in hosting another weather station to output real-time Growing Degree Days and PMRI for the 2020 growing season.

Chapter 4: Socio-economic Considerations for the Success of on-farm Decision Support Tools

Introduction

Weather is the most important factor driving farm production, as it drives plant productivity, planting and harvesting dates, and crop damaging events such as frost, heat waves, and pest and pathogen development. The relatively low-cost weather stations described in Chapter 2 were capable of testing rigorous hypotheses about site-specific weather phenomena. As a result, the stations were able to show weather variability across small spatial scales in an Idaho vineyard, and answer questions about powdery mildew disease pressure that are directly relevant to farm management. Weather variability is also one of the greatest sources of uncertainty in agricultural production systems. For these reasons, farmers should be especially keen on integrating real-time weather data into on-farm operations. Despite enhanced forecasting, warning systems and meteorological technology, adoption of weather-based decision support tools have been slow across many sectors (Blum & Miller, 2019; Uccellini & Ten Hoeve, 2019). Haigh *et al.* (2018) conducted a survey in the southeastern United States and found that nearly half of farmers surveyed did not incorporate weather information into their operations. I argue that the primary factors inhibiting integration of weather information into farm operations are pragmatic concerns associated with the technology itself, the salience of the information, and the perceived value of information to the user's specific application. This synthesis will trace the flow of environmental information from the physical phenomena, to the sensing technologies, through data processing and metrics, and ultimately into the hands of the end decision maker, as shown in Figure 4.1. The uncertainty and challenges associated with each step will be discussed, informed by both my anectodical evidence from working with farmers directly to conduct on-farm research and current literature on the primary socio-economic factors impeding use of weather and climate data.

Data Collection

The first step in collecting meaningful environmental data is in the interaction between sensors and the physical phenomenon of interest. The environment is inherently variable; temperature, wind, humidity, radiation, soil moisture, etc., all vary in time and space. When employed thoughtfully and correctly, sensors can capture the physical events that drive environmental processes. This includes correct sensor placement, selection of appropriate sensing technology, and appropriate data processing to answer questions pertinent to farm management.

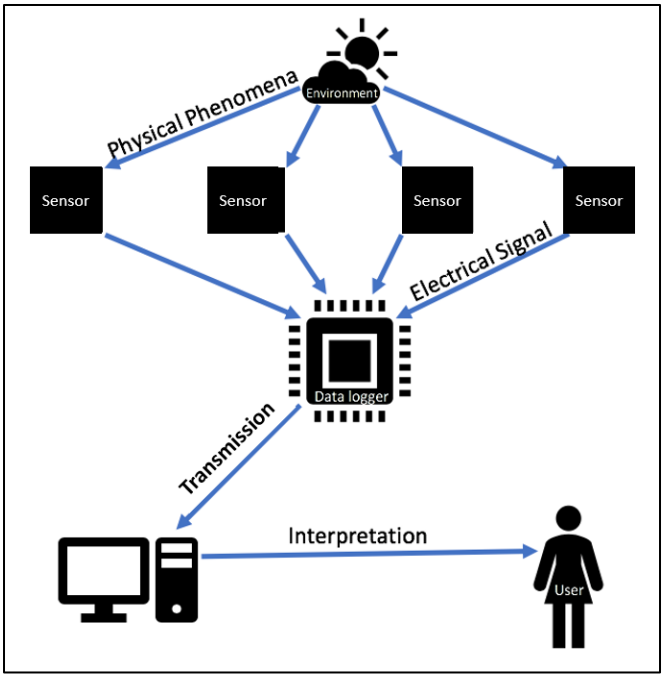

Figure 4.1: Pathways of environmental information

Sensor-Environment Interaction

Sensors should be placed such that they capture the physical event that affect the environmental process of interest, and not some other consequence of the environment. Each sensor performs best under different exposures, and Mahmood et al. (2017) outlined the primary objectives that should be met when placing meteorological instruments. Anemometers should be placed such that they measure the wind profile of interest, and not the air flow diverted from a nearby building or obstruction. Precipitation gauges are placed within a wind shield so that the measurement represents precipitation incident on that unit area, not precipitation blown in from the sides. Soil moisture sensors should be packed tightly in representative soil so that the measurement represents the dielectric permittivity of water within the soil pores, not the air gaps between probes from poor installation. Though these procedures are relatively intuitive, they do add to the practical challenges of hosting environmental monitoring on-farm. For example, placing sensors in field where they are most representative might interfere with other operations and equipment. In the case of the vineyard study, one stations had to be placed at the edge of the field as to not interfere with the tractors' boom. Failure to follow correct installation and setup procedures of the sensors will also lead to erroneous, and unrepresentative data, which in turn decreases the accuracy of data, further contributing to their reluctance towards decision support tools and models.

Sensor Technology

Selecting the appropriate sensor technology is also an important factor in the success of decision support tools. The type of sensor depends on the application, the budget, and the desired level of accuracy. For example, for wind measurements there are two types of anemometers, sonic and cup and vane. Cup and vane anemometers use mechanical components to determine the speed and direction of wind. The major drawback to mechanical anemometers is their limited ability to measure low wind speeds and gust, and maintenance associated with damage to mechanical parts. Sonic anemometer measurements are relatively instantaneous, approximately at the speed of sound, which allow them to capture very low wind speeds, gusts and abrupt changes in direction much more accurately than cup and vane. Sonic anemometers have no moving parts, making them more durable for field applications, thought it comes at a cost. The lowest quality sonic anemometer can be much more expensive than a high-quality cup and vane anemometer.

The site-specific conditions should also be considered when choosing sensor technology. For example, one type of humidity sensing technology is a capacitance hygrometer, which is comprised of a porous polymer between two metallic plates. When the polymer absorbs moisture, the charge between the two plates changes, changing the capacitance of the sensor and hence, the humidity measurement. In this kind of sensing system, anything that impacts the sorption of water into the polymer will affect the accuracy, such as dust or other atmospheric constituents like SO_2. Placing this kind of sensor in a dusty or polluted environment will require frequent maintenance and recalibration to maintain the sensors accuracy. On the contrary, another method of humidity measurement is the psychrometer. Psychrometers use two temperature probes, one placed in dry air (dry bulb), and one wrapped in a wet wick (wet bulb) to measure the temperature under evaporative cooling. The relative humidity can be calculated from these two values using thermodynamic psychrometric equations. The advantage of a psychrometer is that it can withstand dirty environments and water state changes, but psychrometers are often less accurate because the temperature values highly depend on ventilation, wire dimensions, wet wick length, and probe proximity. These two examples highlight the trade-offs that must be considered between upfront cost, maintenance cost, and sensor accuracies when employing on-farm instrumentation.

Information Transmission

After the sensor measurement, the information is transmitted to the user. With the advent of the Internet of Things (IOT), this is commonly done over WIFI or telemetry to a hosted server. For lower cost dataloggers, or areas without WIFI or cell service, data is stored on the device and must be downloaded periodically by the user. The type of data transmission used inherently impacts the

timeliness of the data, and consequently the timing of data-driven decisions. Using the vineyard study as an example, there was no cell service nor WIFI accessibility at the station locations. As a result, data was only downloaded every two weeks. This not only impacted the ability for us to provide real time metrics for the farmer, but also impacted our ability to check on station performance. For example, all the vineyard weather stations lost power in mid-July due to the canopy growing over the solar panel, resulting in a week of lost data. From anecdotal observations, retrieving data manually was one of the biggest complaints about the weather stations deployed in the Ashton study. Similarly, when the low-cost weather stations described in Chapter 1 were presented at an irrigation workshop to regional farmers, the telemetry was one of the greatest concerns. On the contrary, WIFI enabled systems can transmit data almost instantaneously. This real-time information is helpful for a few operations, such as following guidelines for wind speeds when applying pesticides. But in general, farmers are not making decisions on 5-minute time scales. In addition, it is not guaranteed that farms have the infrastructure or capacity to host web-integrated sensors. A recent USDA report showed that in 2019, only 49% of farms used a computer to conduct farm business, and 52% used a smart phone or tablet (*Farm Computer Usage and Ownership*, 2019). That leaves approximately half of the population lacking the essential bandwidth to implement most of these technologies.

Once the raw environmental data has been transmitted, either to a server, an email, or to a personal computer, it should be pre-processed and go through a QA/QC procedure. This can be the most cumbersome part of environmental data collection. Environmental data can be messy, containing missing data, sensor error codes, or incorrect clock times. Real data requires QA/QC procedures to be useful. For cumulative metrics like growing degree days and the PMRI, a few missing data points can render a counter incorrect for the remainder of the season if not filled correctly. Methods for statistically filling missing data can be applied, either by linear interpolation, or regression equations. This introduces another layer of uncertainty in the data and adds complexity that is time consuming and may be impractical for farmers. Ergo, these issues related to sensor technology, telemetry and data processing are one of the first hurdles to integrating on farm data.

Information Use

For environmental data to be successfully interpreted and used by decision makers, it must be salient, packaged in an actionable way, and convey the uncertainty and limitations associated with tool, model or prediction (Kirchhoff, 2013; Prokopy et al., 2017).

Salience

The salience of data refers to its specificity and relevance to a decision maker's unique needs. Currently, regional weather networks provide near real-time data in most locations throughout the

continental US, but these data may not represent local conditions for most locations. Haigh et al. (2018) conducted a survey of farmers in the southeastern United States about their use of private and public weather data. They found that out of the of the farmers who used free, publicly available weather data, only 14% found that the data was very influential to their farming practices Out of the farmers who used both public and private weather data, a majority thought that private weather data was more relevant than public weather data. A comparison of the Powdery Mildew Risk Index calculated using regional weather data compared to on-farm weather data highlights this disparity, Figure 4.2: Comparison of PMRI for on-farm (CCV) vs regional weather stations (DENI)Figure 4.2

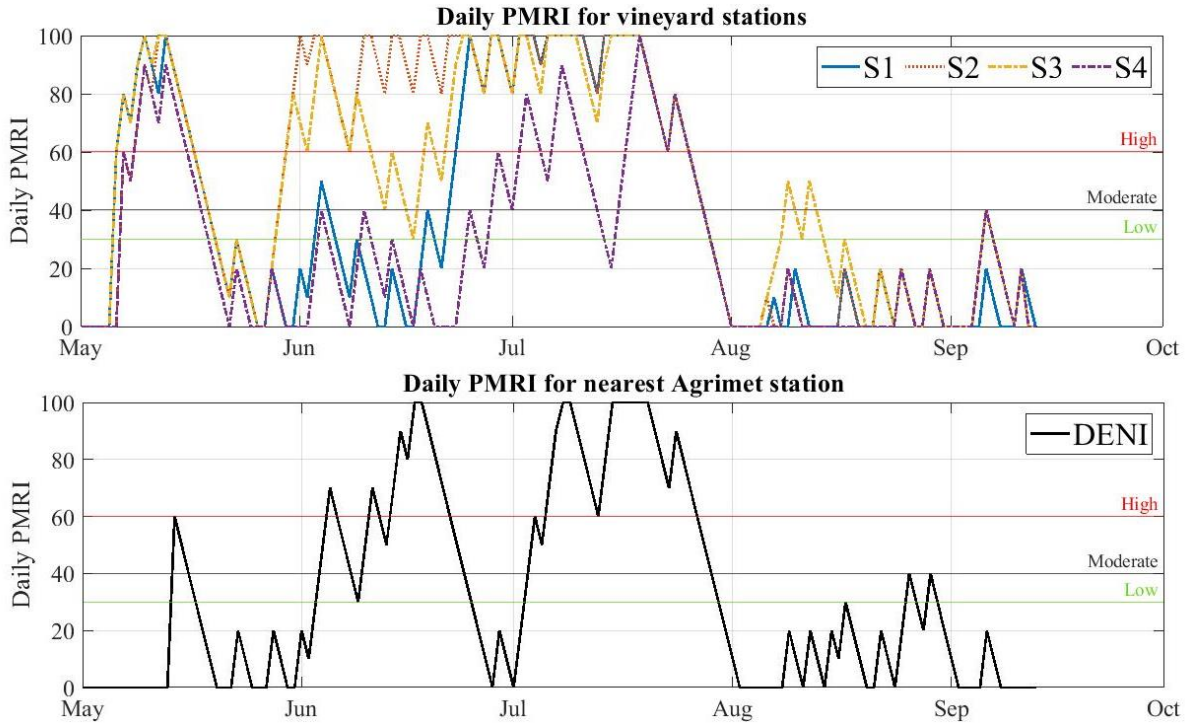

Figure 4.2: Comparison of PMRI for on-farm (CCV) vs regional weather stations (DENI)

The nearest automated weather station to Colter's Creek vineyard is more than 20 miles away at the Dworshak reservoir in Idaho. The first difference to note is the day of initial infection. For the site-specific stations, initial infection began on May 5th for S1, S2 and S3, and May 6th for S4. Initial infection at the Dworshak station was not until May 13th, representing more a week of disease risk information the farmer would be missing. The DENI data follow similar trends, but daily values of PMRI vary substantially from the vineyard stations, particularly from S3 and S2.

Actionable Data Packaging

One way to improve the packaging of environmental data is by reducing the dimensionality of raw environmental data by compiling it into a single data metric. As shown in the vineyard study, air

temperature data collected on a 5-minute interval can be transformed into three different data products which inform unique crop processes: growing degree days, reference ET, and the powdery mildew risk index. Cumulative data products like these provide a single value, often on a daily time-step, that can be compared to established thresholds which inform action. For example, the P-M reference ET equation integrates a relatively large number of observations on air temperature, wind speed, humidity and solar radiation conditions over the course of day into a single value that informs weather related crop water demand. The PMRI provides information on the risk of powdery mildew infection for a single day based on temperature trends from the many days prior. By presenting this data in graphical form and adding thresholds which inform fungicide application, a decision maker can both learn their present disease risk and act on it from one glance. Further, reporting the PMRI at multiple locations incorporators spatial variability into the metric, allowing for management strategies to be resolved to field or sub-field scales.

Many people are best able to utilize information visually, as a result maps are another useful way of data communication. Prokopy et al. (2017) conducted a study on farmers needs in relation to agricultural decision support tools. One of the major takeaways from focus groups was that visualization of data in maps was the most useful for farmers to interpret. Similarly, from my experience working with the vineyard manager, his interest peaked when he was presented with maps of field variability. Maps are also another way of dimensionality reduction. A single point on a map can contain spatial, temporal, and variable information. For example, the stress index maps created in the vineyard project combines information on instantaneous air temperature, relative humidity, canopy temperature, location, time as well as seasonal averages from the near-by weather stations time-series. A single point conveys six-dimensional data to a farmer in a digestible way. These kinds of data products are useable, efficient, and actionable. Though creation of these data products is not trivial, this is the responsibility of researchers and extension to find ways of effectively communicating complex processes to farmers.

Conveying Uncertainty

The end users of the data products need to be equipped with all the tools necessary to make the most informed judgement. This includes communicating the uncertainty and limits associated with the data, prediction, or model, as well as the uncertainty related to their specific decision context (Kirchhoff, 2013). Again, this is most digestible to farmers when presented visually, such as use of error bars and uncertainty bounds around the data. Many studies have also found that interaction between the producers of information and the users of information can help mitigate perceptions of uncertainty, or inaccuracies of the data (Kirchhoff, 2013; Kirchhoff et al., 2013; Prokopy et al., 2017;

Uccellini & Ten Hoeve, 2019). These discussions should be facilitated through extension services and workshops where the data production process is thoroughly explained, including sources of uncertainty. Similarly, when reporting environmental data from regional weather networks or when reporting to farm managers, enough information should be given about the monitoring set up and environmental conditions so that users can judge the credibility and relevancy of environmental data (Allen et al., 2011b). Appropriately communicating uncertainty in scientific models and will help increase decision makers confidence in their application of these tools.

Value of Information

The previous sections highlight key challenges and areas of improvement related to the collection and reporting of environmental data products and decision support tools. However, when it comes to the adoption of such tools, we must also consider the perceived value of information to the farmers, and the associated risks farmers face that might impede their willingness to incorporate environmental data into their operation.

Perceived Risks

Perceived risk plays a role in the willingness of decision makers to use weather and climate data. Attitudes towards risk also vary substantially across individuals, over time, and with experience (Kirchhoff et al., 2013). In general, when the perceived risk of weather-related damage is high, decision makers are more likely to find utility in weather information. For example, the most important factor in adaptive behavior for farmer's in the corn belt was found to be individual perception of on-farm risks such as drought, flooding, and crop disease (Prokopy et al., 2017). They also found that the farmer's underlying beliefs about the climate change also had a significant impact on how they manage their farms. The more the farmer believes climate change is caused by human activity, the more likely they are to use of information technology compared to those who did not believe climate change is caused by human activity. Similarly, Kirchhoff et al. (2013) found that water managers who expect to face problems from the climate in the next decade were much more likely to use climate forecasts to inform decision-making. In summary, farmers that are more climate aware, and anticipate weather related damages to their crops are more willing to manage risk with weather and climate information. However, perceived risk of weather-related damages and its influence on adoption of weather-driven practices differs from the actual risk of employing sensor-driven management.

Potential economic benefits of decision support tools and precision farming ultimately stem from reducing the cost of inputs, such as irrigation water, fertilizers, or pesticides. Though use of these tools comes with increased risk (Sadler et al., 2005). Haigh *et al.* (2018) found that farmers were

particularly doubtful that weather information from any source, private or public, would reduce their financial risks. Depending on the application of the decision support tool, the risk associated with incorrect crop management can curtail use of sensor data. For example, sensor-based irrigation scheduling has some risk associated with it, but it is asymmetrically distrusted throughout the season (Food and Agriculture Organization of the United Nations, 2002). In the early season, there is greater risk associated with under or over-watering crops, particularly for annual crops. Underwatering can lead to yield reduction, unwanted crop stress, and severely impact the crop quality. This is particularly critical for high value crops like fruits and nuts, where the market price of high-quality fruit much outweighs the marginal cost of applying water (Knox et al., 2012). Overwatering can be costly in the form of pumping costs, facilitate disease development, and be environmentally unsustainable. For crops like grapes, which are intentionally stressed at the end of the season to improve fruit composition (Herrera et al., 2017), the risk of underwatering diminishes later in the season.

When evaluating the farmer's perception of risk related to irrigation, it is also important to consider how the farmer defines irrigation efficiency. In agriculture, the term efficiency can have different meanings. A survey in England found that 63% of farmers surveyed considered water use efficiency to mean "applying the right amount of water at the right time in the right place". Conversely, water regulators view water use efficiency from a social-ecological perspective where their goal is to manage abstractions to sustain the entire water environment and local business (Knox et al., 2012). From a water manager's perspective, the non-consumed "losses" at a field scale such as runoff and deep percolation lead to return flows to the environment which can be reused basin wide. However, from a farmer's perspective increased irrigation efficiency often means reducing runoff and deep percolation. Rather than reducing the water abstracted, water savings at one field can be applied to another, or the irrigated area can be expanded to increase productions. Hence, water saved at a farm scale does not mean water saved at a watershed scale.

As another example, the risk associated with disease management is consistent throughout the early and middle parts of growing season. As shown in Chapter 3, powdery mildew disease risk tends to diminish at the end of the season. If a farmer does not sufficiently apply pesticides during high risk periods, they run the risk of losing their entire year's crop to disease, or in the case of perineal crops, be forced to eradicate entire blocks of vineyards or orchards which will affect them for years to come. The marginal cost of pesticide application is also much greater than the marginal cost of water, which increases the financial risk associated with over-spraying. Hence, trusting technology for these kinds of high stakes applications is risky.

Value Perceptions

In some cases, farmers might perceive the value of information from on-farm sensors to out-weigh the potential risks. The value of information technology is difficult to quantify, as it requires observing a counterfactual. The difference in the farmer's outcome with and without use of decision support tools cannot be measured, but it can be theoretically modeled. Galioto et al. (2017) derived an economic model to determine the value of information for precision irrigation practices. The value of information was modeled as the difference between maximum profit from the sensor informed outcome and the maximum profit from the outcome without the sensor information. Two main relationships were found; the value of information to a farmer increases with increased field heterogeneity and the informed action provides more profitable outcomes when the probability of the sensors to correctly predict the phenomena is greater than the probability of the farmer to correctly react. These relationships are shown in Figure 4.3.

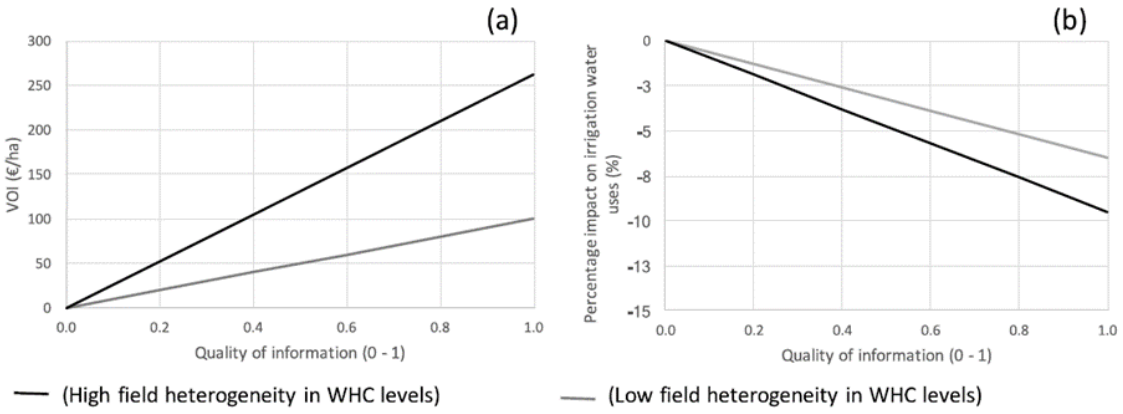

Figure 4.3: Compares the value of information (a) and impact on irrigation water use (b) between fields with high and low heterogeneity as a function of information quality from Galioto et al., (2020)

If the number of distinct management zones is one of the primary factors adding to the value of sensor information, then identification of such zones is of utmost importance. This is another practical obstacle to adoption of decision support tools. Accurate identification of management zones is laborious and expensive. It involves large field campaigns to adequately sample across spatial scales, and long periods of monitoring to detect significant differences in temporal patterns. Compounding this, each variable input is likely to have different management zones (Sadler et al., 2005). For example, irrigation zones are likely to be different than pesticide zones, which will be different than nutrient zones. Though this effort is rarely employed in reality, it goes to show the degree of information necessary to accurately use and benefit from decision support tools. It highlights cracks in the system that might lead to models performing unsatisfactory in field compared to research experiments, and further dissuade farmers from trusting decision support tools.

The number management zones that can be monitored is limited by the number of sensors a farmer can afford to deploy. Consequently, cheaper sensors usually have lower accuracy. As Galioto et al., (2017) pointed out, the value of information from decision support tools is a function of the accuracy of the sensor, or the probability of the sensor to correctly predict the natural state. The model accuracy is the culmination of sensor accuracy, appropriate data processing, and the accuracy of fundamental physics and assumptions used to interpret the physical phenomena. When multiple sensors are coupled to provide more sophisticated metrics like potential evapotranspiration, this uncertainty in the system compounds. One way to way to reduce the risk of misinformed management from decision support tools, and increase their potential value, is by correct sensor set up, as described in the first section of this chapter. Sensor placement, sensor accuracy, and representativeness all contribute to overall ability of the data to provide meaningful metrics. There are real trade-offs between the number of management zones, quality of sensors, and ultimate economic savings from adoption of precision agriculture technology and decision support tools.

The cost analysis presented in Chapter 2 shows that the cost associated with using weather information to support disease management is about $380/acre per year. This estimate includes the cost of placing four weather stations across a 35-acre vineyard. Given the vineyard is producing the average yield and fruit quality for the state of Idaho, the potential losses from a disease outbreak is on the order of $1,800/acre. However, the results in Chapter 3 show that weather does not vary substantially between Station 1 and Station 3, indicating that only one weather station is necessary to capture the weather conditions in that vineyard block. Given that there were also two vineyard blocks that did not have a weather station, I would suggest that five weather stations be placed in the 35-acre vineyard to provide the best coverage. Additionally, results from the Powdery Mildew Risk Index indicate that the farmer should spray weekly from May to July, pushing the number of spray applications from 8 to 16. If a farmer was solely using the weather data to inform fungicide application, these adjustments would increase the cost of disease management over the course of a growing season to $675/acre.

Taking the difference between the cost of management and the potential cost of disease, this shows that value of weather information could be as much as $1125/acre, given the PMRI model is accurate enough to eliminate the risk of disease. As observed in the vineyard study, the farmer’s current disease management strategy is effective, and there was not a powdery mildew outbreak in 2019. However, climate change scenarios predict that regional weather patterns will become more variable. As such. the ability for a farmer to correctly predict weather driven processes such as irrigation

demand and disease will become more challenging. This simple economic estimate provides a first cut approximation on the cost of information to help mitigate risk.

Conclusion

There is a paradox between the spatial representation of information, the accuracy of information, and the price of information. Different approaches of environmental monitoring have different relative values. Chapter 2 showed that the lower cost ($16) SHT-31 sensors are not as accuracy as the higher quality ATMOS-41 sensors. Calibration results shown an average r-square of 0.95 and 0.96 for relative humidity and temperature measurements, respectively. However, the value of each of these sensors depends on the farmer's specific needs. In the case, of the vineyard study, we placed four sensor stations that used low-cost data loggers with relatively high-quality sensors. Data provided by these stations showed that weather variability varied across small scales, and as a result we can differentiate three potential disease management zones. Had we placed many lower cost sensors, such as the SHT-31 temperature and humidity sensors, we might have observed more disparate microclimates. Though, the spatial scales over which unique disease management regimes can be applied are limited by operational constraints. As discussed in the chapter, when the application is high risk, as is the case with disease management, accuracy of the model becomes a priority. For these reasons, a fewer number of high-quality sensors is likely the best choice for weather-based disease models.

The study at Colter's Creek also showed variable growing degree days across the four locations. Growing degree days trackers are cumulative models that are not very sensitive to measurement accuracy. For example, GDDs calculated from a temperature sensor with an accuracy of ±0.5°C compared to a sensor with ±0.1°C will track accumulation of heat relatively equally. Management decisions based of GDDs, such as harvesting dates, can be applied across small spatial scales, especially in vineyards where grapes are harvested by hand. For this application, I would recommend many distributed low-cost temperature sensors compared to a few high-quality sensors. The accuracies of the low-cost sensors should be more than adequate to improve decision making for this application. When considering the alternative of farmers using data from regional weather stations to track growing degree days, disease risk indices, or reference evapotranspiration, any on-farm measurement, independent of quality, will be much more useful and representative.

Clearly, there is a long way to go before every farmer is making real-time, precise decisions on crop management from site-specific weather data. Currently, the major socio-economic factors inhibiting the adoption of on farm weather data are information credibility, on-farm practicality, and the risk of using data to inform critical, high stakes management decisions. Trade-offs between temporal and

spatial resolution, information costs, and information quality should all be considered when evaluating the value of information technology to decision makers. However, I believe sub-optimal data is better than no data. Continuous and spatially distributed data adds to the wealth of information a farmer can use to learn about their field. Whether they choose to use these insights to precisely target management will depend on their individual perceptions of risk and expected economic utility. These socio-economic considerations for the success of decision support tools extend beyond agricultural applications. Issues related to the practicality, salience, and value of collecting, analyzing and employing environmental data are relevant across many sectors. Forest management, water resource management, and environmental protection agencies can all benefit from climate and weather-based decision support tools.

Literature Cited

Allen, R. G., Pereira, L. S., Howell, T. A., & Jensen, M. E. (2011a). Evapotranspiration information reporting: I. Factors governing measurement accuracy. *Agricultural Water Management*, *98*(6), 899–920. https://doi.org/10.1016/j.agwat.2010.12.015

Allen, R. G., Pereira, L. S., Howell, T. A., & Jensen, M. E. (2011b). Evapotranspiration information reporting: II. Recommended documentation. *Agricultural Water Management*, *98*(6), 921–929. https://doi.org/10.1016/j.agwat.2010.12.016

ASCE Manual 70 – Second Edition: Evaporation, Evapotranspiration and Irrigation Requirements. (2015). *2015 ASABE / IA Irrigation Symposium: Emerging Technologies for Sustainable Irrigation - A Tribute to the Career of Terry Howell, Sr. Conference Proceedings*, 1–16. https://doi.org/10.13031/irrig.20152143358

ATMOS 41—Correction of air temperature measurements from a radiation-exposed sensor. (n.d.). https://www.metergroup.com/environment/articles/atmos-41-correction-air-temperature-measurements-radiation-exposed-sensor/

Austin, C. N., & Wilcox, W. F. (2011). Effects of Fruit-Zone Leaf Removal, Training Systems, and Irrigation on the Development of Grapevine Powdery Mildew. *American Journal of Enology and Viticulture*, *62*(2), 193–198. https://doi.org/10.5344/ajev.2010.10084

Bailey, B. N., Stoll, R., Pardyjak, E. R., & Miller, N. E. (2016). A new three-dimensional energy balance model for complex plant canopy geometries: Model development and improved validation strategies. *Agricultural and Forest Meteorology*, *218–219*, 146–160. https://doi.org/10.1016/j.agrformet.2015.11.021

Baldocchi, D. (2014). Measuring fluxes of trace gases and energy between ecosystems and the atmosphere—The state and future of the eddy covariance method. *Global Change Biology*, *20*(12), 3600–3609. https://doi.org/10.1111/gcb.12649

Bélanger, M. -C., Roger, J. -M., Cartolaro, P., Viau, A. A., & Bellon-Maurel, V. (2008). Detection of powdery mildew in grapevine using remotely sensed UV-induced fluorescence. *International Journal of Remote Sensing*, *29*(6), 1707–1724. https://doi.org/10.1080/01431160701395245

Blum, A. G., & Miller, A. (2019). Opportunities for Forecast-Informed Water Resources Management in the United States. *Bulletin of the American Meteorological Society*, *100*(10), 2087–2090. https://doi.org/10.1175/BAMS-D-18-0313.1

Calonnec, A., Cartolaro, P., Poupot, C., Dubourdieu, D., & Darriet, P. (2004). Effects of Uncinula necator on the yield and quality of grapes (Vitis vinifera) and wine. *Plant Pathology*, *53*(4), 434–445. https://doi.org/10.1111/j.0032-0862.2004.01016.x

Caubel, J., Launay, M., Cortazar-Atauri, I. G., Ripoche, D., Huard, F., Buis, S., & Brisson, N. (2013). A new integrated approach to assess the impacts of climate change on grapevine fungal diseases: The coupled MILA-STICS model. *Journal International Des Sciences de La Vigne et Du Vin Special Laccave*, 45–54.

Chakraborty, S., Tiedemann, A. V., & Teng, P. S. (2000). Climate change: Potential impact on plant diseases. *Environmental Pollution*, *108*(3), 317–326. https://doi.org/10.1016/S0269-7491(99)00210-9

Choudhury, R. A., Mahaffee, W. F., McRoberts, N., & Gubler, W. D. (2018). *Modeling Uncertainty in Grapevine Powdery Mildew Epidemiology Using Fuzzy Logic* [Preprint]. Epidemiology. https://doi.org/10.1101/264622

Coble, K. H., Mishra, A. K., Ferrell, S., & Griffin, T. (2018). Big Data in Agriculture: A Challenge for the Future. *Applied Economic Perspectives and Policy*, *40*(1), 79–96. https://doi.org/10.1093/aepp/ppx056

Davis, S. L., & Dukes, M. D. (2010). Irrigation scheduling performance by evapotranspiration-based controllers. *Agricultural Water Management*, *98*(1), 19–28. https://doi.org/10.1016/j.agwat.2010.07.006

Evans, R. G., & King, B. A. (2012). Site Specific Sprinkler Irrigation in a Water Limited Future. *American Society of Biological and Agricultural Engineers*, *55*, 493–504.

Farm Computer Usage and Ownership. (2019). USDA National Agricultural Statistics Service. https://downloads.usda.library.cornell.edu/usda-esmis/files/h128nd689/8910k592p/qz20t442b/fmpc0819.pdf

Fernandez-Cornejo, J., Nehring, R., Osteen, C., Wechsler, S., Martin, A., & Vialou, A. (2014). *Pesticide Use in U.S. Agriculture: 21 Selected Crops, 1960-2008* (Economic Research Service Economic Information Bulletin No. 124). United States Department of Agriculture. https://www.ers.usda.gov/webdocs/publications/43854/46734_eib124.pdf?v=0

Fidelibus, M., El-kereamy, A., Haviland, D., Hembree, K., Zhuang, G., Steward, D., & Sumner, D. A. (2018). *Table Grapes-Sheegene-21 Early Maturing Costs & Returns Study*. UC DAVIS DEPARTMENT OF AGRICULTURAL AND RESOURCE ECONOMICS.

Fisher, D. K., & Gould, P. J. (2012). Open-Source Hardware Is a Low-Cost Alternative for Scientific Instrumentation and Research. *Modern Instrumentation*, *01*(02), 8–20. https://doi.org/10.4236/mi.2012.12002

Fisher, D. K., & Kebede, H. (2010). A low-cost microcontroller-based system to monitor crop temperature and water status. *Computers and Electronics in Agriculture*, *74*(1), 168–173. https://doi.org/10.1016/j.compag.2010.07.006

Food and Agriculture Organization of the United Nations (Ed.). (2002). *Deficit irrigation practices*. Food and Agriculture Organization of the United Nations.

Food and Agriculture Organization of the United Nations (Ed.). (2017). *The future of food and agriculture: Trends and challenges*. Food and Agriculture Organization of the United Nations.

Gadoury, D. M., Seem, R. C., Pearson, R. C., Wilcox, W. F., & Dunst, R. M. (2001). Effects of Powdery Mildew on Vine Growth, Yield, and Quality of Concord Grapes. *Plant Disease*, *85*(2), 137–140. https://doi.org/10.1094/PDIS.2001.85.2.137

Gadoury, D. M., Seem, R. C., Wilcox, W. F., Henick-Kling, T., Conterno, L., Day, A., & Ficke, A. (2007). Effects of Diffuse Colonization of Grape Berries by *Uncinula necator* on Bunch Rots, Berry Microflora, and Juice and Wine Quality. *Phytopathology*, *97*(10), 1356–1365. https://doi.org/10.1094/PHYTO-97-10-1356

Galioto, F., Chatzinikolaou, P., Raggi, M., & Viaggi, D. (2020). The value of information for the management of water resources in agriculture: Assessing the economic viability of new methods to schedule irrigation. *Agricultural Water Management*, *227*, 105848. https://doi.org/10.1016/j.agwat.2019.105848

Galioto, F., Raggi, M., & Viaggi, D. (2017). Assessing the Potential Economic Viability of Precision Irrigation: A Theoretical Analysis and Pilot Empirical Evaluation. *Water*, *9*(12), 990. https://doi.org/10.3390/w9120990

Gamon, J. A., Peñuelas, J., & Field, C. B. (1992). A narrow-waveband spectral index that tracks diurnal changes in photosynthetic efficiency. *Remote Sensing of Environment*, *41*(1), 35–44. https://doi.org/10.1016/0034-4257(92)90059-S

Gitelson, A. A., Keydan, G. P., & Merzlyak, M. N. (2006). Three-band model for noninvasive estimation of chlorophyll, carotenoids, and anthocyanin contents in higher plant leaves. *Geophysical Research Letters*, *33*(11), L11402. https://doi.org/10.1029/2006GL026457

Gjanci, J., & Chowdhury, M. (2008). Investigating issues of on-chip voltage regulator in nanoscale integrated circuits. *2008 International Conference on Microelectronics*, 123–126. https://doi.org/10.1109/ICM.2008.5393555

Griffin, T. W., Miller, N. J., Bergtold, J., Shanoyan, A., Sharda, A., & Ciampitti, I. A. (2017). Farm's Sequence of Adoption of Information-intensive Precision Agricultural Technology. *Applied Engineering in Agriculture*, *33*(4), 521–527. https://doi.org/10.13031/aea.12228

Gubler, W. D., Rademacher, M. R., & Vasquez, S. J. (1999). Control of Powdery Mildew Using the UC Davis Powdery Mildew Risk Index. *APSnet Feature Articles*. https://doi.org/10.1094/APSnetFeature-1999-0199

Gultepe, I., Fernando, H. J. S., Pardyjak, E. R., Hoch, S. W., Silver, Z., Creegan, E., Leo, L. S., Pu, Z., De Wekker, S. F. J., & Hang, C. (2016). An Overview of the MATERHORN Fog Project: Observations and Predictability. *Pure and Applied Geophysics*, *173*(9), 2983–3010. https://doi.org/10.1007/s00024-016-1374-0

Gunawardena, N., Pardyjak, E. R., Stoll, R., & Khadka, A. (2018). Development and evaluation of an open-source, low-cost distributed sensor network for environmental monitoring applications. *Measurement Science and Technology*, *29*(2), 024008. https://doi.org/10.1088/1361-6501/aa97fb

H. J. Farahani, T. A. Howell, W. J. Shuttleworth, & W. C. Bausch. (2007). Evapotranspiration: Progress in Measurement and Modeling in Agriculture. *Transactions of the ASABE*, *50*(5), 1627–1638. https://doi.org/10.13031/2013.23965

Haigh, T., Koundinya, V., Hart, C., Klink, J., Lemos, M., Mase, A. S., Prokopy, L., Singh, A., Todey, D., & Widhalm, M. (2018). Provision of Climate Services for Agriculture: Public and Private Pathways to Farm Decision-Making. *Bulletin of the American Meteorological Society*, *99*(9), 1781–1790. https://doi.org/10.1175/BAMS-D-17-0253.1

Hang, C., Nadeau, D. F., Jensen, D. D., Hoch, S. W., & Pardyjak, E. R. (2016). Playa Soil Moisture and Evaporation Dynamics During the MATERHORN Field Program. *Boundary-Layer Meteorology*, *159*(3), 521–538. https://doi.org/10.1007/s10546-015-0058-0

Hennemuth, B., Bender, S., Dreier, N., Keup-Thiel, E., Krüger, O., Mudersbach, C., Radermacher, C., & Schoetter, R. (2013). *Statistical methods for the analysis of simulated and observed climate data, applied in projects and institutions dealing with climate change impact and adaptation* (Technical CSC Report 13). Climate Service Center. https://www.climate-service-center.de/imperia/md/content/csc/projekte/csc-report13_englisch_final-mit_umschlag.pdf

Herrera, J. C., Hochberg, U., Degu, A., Sabbatini, P., Lazarovitch, N., Castellarin, S. D., Fait, A., Alberti, G., & Peterlunger, E. (2017). Grape Metabolic Response to Postveraison Water Deficit Is Affected by Interseason Weather Variability. *Journal of Agricultural and Food Chemistry*, *65*(29), 5868–5878. https://doi.org/10.1021/acs.jafc.7b01466

Hildebrandt, A., Guillamón, M., Lacorte, S., Tauler, R., & Barceló, D. (2008). Impact of pesticides used in agriculture and vineyards to surface and groundwater quality (North Spain). *Water Research*, *42*(13), 3315–3326. https://doi.org/10.1016/j.watres.2008.04.009

Ibrahim Musa, A. (2018). Micro-controller Based Mobile Weather Monitor System. *American Journal of Embedded Systems and Applications*, *6*(1), 23. https://doi.org/10.11648/j.ajesa.20180601.14

Irrigation & Water Use. (2019). USDA Economic Research Service. https://www.ers.usda.gov/topics/farm-practices-management/irrigation-water-use/

Jensen, D. D., Nadeau, D. F., Hoch, S. W., & Pardyjak, E. R. (2017). The evolution and sensitivity of katabatic flow dynamics to external influences through the evening transition: Effect of External Influences on Katabatic Flow. *Quarterly Journal of the Royal Meteorological Society*, *143*(702), 423–438. https://doi.org/10.1002/qj.2932

Kirchhoff, C. J. (2013). Understanding and enhancing climate information use in water management. *Climatic Change*, *119*(2), 495–509. https://doi.org/10.1007/s10584-013-0703-x

Kirchhoff, C. J., Carmen Lemos, M., & Dessai, S. (2013). Actionable Knowledge for Environmental Decision Making: Broadening the Usability of Climate Science. *Annual Review of Environment and Resources*, *38*(1), 393–414. https://doi.org/10.1146/annurev-environ-022112-112828

Knox, J. W., Kay, M. G., & Weatherhead, E. K. (2012). Water regulation, crop production, and agricultural water management—Understanding farmer perspectives on irrigation efficiency. *Agricultural Water Management*, *108*, 3–8. https://doi.org/10.1016/j.agwat.2011.06.007

Mahmood, R., Boyles, R., Brinson, K., Fiebrich, C., Foster, S., Hubbard, K., Robinson, D., Andresen, J., & Leathers, D. (2017). Mesonets: Mesoscale Weather and Climate Observations for the United States. *Bulletin of the American Meteorological Society*, *98*(7), 1349–1361. https://doi.org/10.1175/BAMS-D-15-00258.1

Marshall, M., Thenkabail, P., Biggs, T., & Post, K. (2016). Hyperspectral narrowband and multispectral broadband indices for remote sensing of crop evapotranspiration and its components (transpiration and soil evaporation). *Agricultural and Forest Meteorology*, *218–219*, 122–134. https://doi.org/10.1016/j.agrformet.2015.12.025

Mase, A. S., & Prokopy, L. S. (2014). Unrealized Potential: A Review of Perceptions and Use of Weather and Climate Information in Agricultural Decision Making. *Weather, Climate, and Society*, *6*(1), 47–61. https://doi.org/10.1175/WCAS-D-12-00062.1

Monteith, J. L. (1965). Evaporation and environment. *Symposia of the Society for Experimental Biology*, *19*, 205–234.

Natural Resources Conservation Service, United States Department of Agriculture. (2017, August 21). *Web Soil Survey*. Web Soil Survey. https://websoilsurvey.sc.egov.usda.gov/App/WebSoilSurvey.aspx

Oerke, E.-C. (Ed.). (1994). *Crop production and crop protection: Estimated losses in major food and cash crops*. Elsevier.

Oerke, Erich-Christian, Herzog, K., & Toepfer, R. (2016). Hyperspectral phenotyping of the reaction of grapevine genotypes to *Plasmopara viticola*. *Journal of Experimental Botany*, *67*(18), 5529–5543. https://doi.org/10.1093/jxb/erw318

Oppelt, N., & Mauser, W. (2004). Hyperspectral monitoring of physiological parameters of wheat during a vegetation period using AVIS data. *International Journal of Remote Sensing*, *25*(1), 145–159. https://doi.org/10.1080/0143116031000115300

Ozelkan, E., Karaman, M., Candar, S., Coskun, Z., & Ormeci, C. (2015). Investigation of grapevine photosynthesis using hyperspectral techniques and development of hyperspectral band ratio indices sensitive to photosynthesis. *Journal of Environmental Biology*, *36 Spec No*, 91–100.

Palmer, P., & Hamel, J. (2009). *QUALITY ASSURANCE PROCEDURES FOR RECLAMATION'S AGRIMET WEATHER STATION NETWORK*. https://westernsnowconference.org/sites/westernsnowconference.org/PDFs/2009Palmer.pdf

Penman, H. L. (1948). Natural Evaporation from Open Water, Bare Soil, and Grass. *JSTOR*, 120–145.

Peñuelas, J., Filella, I., Biel, C., Serrano, L., & Savé, R. (1993). The reflectance at the 950–970 nm region as an indicator of plant water status. *International Journal of Remote Sensing*, *14*(10), 1887–1905. https://doi.org/10.1080/01431169308954010

Perry, C., Steduto, P., Allen, Richard. G., & Burt, C. M. (2009). Increasing productivity in irrigated agriculture: Agronomic constraints and hydrological realities. *Agricultural Water Management*, *96*(11), 1517–1524. https://doi.org/10.1016/j.agwat.2009.05.005

Plant Health and Food Security (I7829EN/1/09.17). (2017). International Plant Protection Convention (IPPC). http://www.fao.org/3/a-i7829e.pdf

Precision Agriculture in the 21st Century: Geospatial and Information Technologies in Crop Management. (1997). National Academies Press. https://doi.org/10.17226/5491

Prokopy, L. S., Carlton, J. S., Haigh, T., Lemos, M. C., Mase, A. S., & Widhalm, M. (2017). Useful to Usable: Developing usable climate science for agriculture. *Climate Risk Management*, *15*, 1–7. https://doi.org/10.1016/j.crm.2016.10.004

Quevedo, H., & Gonzalez, G. A. (2017). Non-normal Distribution of Temperatures in the United States of America during 1895-2016: A Challenge to the Central Limit Theorem. *Pinachle Environment & EarthSciences*, *4*(1).

Rumpf, T., Mahlein, A.-K., Steiner, U., Oerke, E.-C., Dehne, H.-W., & Plümer, L. (2010). Early detection and classification of plant diseases with Support Vector Machines based on hyperspectral reflectance. *Computers and Electronics in Agriculture*, *74*(1), 91–99. https://doi.org/10.1016/j.compag.2010.06.009

Sadler, E. J., Evans, R. G., Stone, K. C., & Camp, C. R. (2005). Opportunities for conservation with precision irrigation. *Journal of Soil and Water Conservation*, *60*(6).

Simon, H., Lindén, J., Hoffmann, D., Braun, P., Bruse, M., & Esper, J. (2018). Modeling transpiration and leaf temperature of urban trees – A case study evaluating the microclimate model ENVI-met against measurement data. *Landscape and Urban Planning*, *174*, 33–40. https://doi.org/10.1016/j.landurbplan.2018.03.003

Smith, K. (2014, July). *EnviroDIY Arduino SDI-12*. GitHub. https://github.com/EnviroDIY/Arduino-SDI-12/issues/8

Stoll, M., Schultz, H. R., Baecker, G., & Berkelmann-Loehnertz, B. (2008). Early pathogen detection under different water status and the assessment of spray application in vineyards through the use of thermal imagery. *Precision Agriculture*, *9*(6), 407–417. https://doi.org/10.1007/s11119-008-9084-y

Tantalaki, N., Souravlas, S., & Roumeliotis, M. (2019). Data-Driven Decision Making in Precision Agriculture: The Rise of Big Data in Agricultural Systems. *Journal of Agricultural & Food Information*, *20*(4), 344–380. https://doi.org/10.1080/10496505.2019.1638264

Uccellini, L. W., & Ten Hoeve, J. E. (2019). Evolving the National Weather Service to Build a Weather-Ready Nation: Connecting Observations, Forecasts, and Warnings to Decision-Makers through Impact-Based Decision Support Services. *Bulletin of the American Meteorological Society*, *100*(10), 1923–1942. https://doi.org/10.1175/BAMS-D-18-0159.1

van Niekerk, J. M., E. STREVER, A., du TOIT, P. G., HALLEEN, F., & FOURIE, P. H. (2011). Influence of water stress on Botryosphaeriaceae disease expression in grapevines. *Phytopathol. Mediterr.*, *50*, 151–156.

Wolfert, S., Ge, L., Verdouw, C., & Bogaardt, M.-J. (2017). Big Data in Smart Farming – A review. *Agricultural Systems*, *153*, 69–80. https://doi.org/10.1016/j.agsy.2017.01.023

Appendix A: P-M Reference ET Calculation

The equation used to calculate the standardized reference ET for alfalfa reference (ET_{rs}) is as follows:

$$ET_{rs} = \frac{0.408\Delta(R_n - G) + \gamma * \left(\frac{C_n}{T + 273}\right) * u_2(e_s - e_a)}{\Delta + \gamma(1 + C_d u_2)}$$

where Δ is the slope of the saturation vapor pressure curve,

$$\Delta = \frac{2503 * \exp\left(\frac{17.27T}{T + 237.3}\right)}{(T + 237.s)^2}$$

and γ is the psychometric constant,

$$\gamma = 0.000665 * P_{atm}$$

The saturation vapor pressure, e_s is a function of air temperature,

$$e_s(\mathrm{T}) = 0.6108 * \exp\left(\frac{17.27T}{T + 237.3}\right)$$

and the actual vapor pressure, e_a, is calculated from the percent relative humidity measurement,

$$e_a = \frac{\%RH}{e_s} * 100$$

R_n is the net radiation which is equal to the net longwave radiation subtracted by the net shortwave radiation:

$$R_n = (R_{sw} + R_{lw})_{incoming} - (R_{sw} + R_{lw})_{outgoing}$$

Ground flux density, G is the radiation flux into the soil and can be assumed negligible on daily time steps, u_2 is the horizontal wind speed measured at 2 meters, and T is the air temperature in degrees Celsius. For the alfalfa reference on a daily time step C_n = 1600 and $C_d = 0.38$.